Solar system science with the Orbiting Astronomical Satellite Investigating Stellar Systems (OASIS) observatory

Anderson, C.M.; Biver, N.; Bjoraker, G.L.; Cavalié, T.; Chin, G.; DiSanti, M.A.; ... ; Walker, C.K.

Space Science Reviews (2022) 218:43
https://doi.org/10.1007/s11214-022-00911-5

Solar System Science with the Orbiting Astronomical Satellite Investigating Stellar Systems (OASIS) Observatory

Carrie M. Anderson[1] · Nicolas Biver[2] · Gordon L. Bjoraker[1] · Thibault Cavalié[2,3] · Gordon Chin[1] · Michael A. DiSanti[1] · Paul Hartogh[4] · Alexander Tielens[5] · Christopher K. Walker[6]

Received: 9 March 2022 / Accepted: 15 June 2022 / Published online: 18 July 2022

Abstract

The overarching theme of the *Orbiting Astronomical Satellite for Investigating Stellar Systems (OASIS)*, an Astrophysics MIDEX-class mission concept, is *Following water from galaxies, through protostellar systems, to Earth's oceans*. The *OASIS science objectives* address fundamental questions raised in "Pathways to Discovery in Astronomy and Astrophysics for the 2020s (National Academies of Sciences and Medicine, Pathways to Discovery in Astronomy and Astrophysics for the 2020s, 2021, https://doi.org/10.17226/26141, https://www.nap.edu/catalog/26141/pathways-to-discovery-in-astronomy-and-astrophysics-for-the-2020s)" and in "Enduring Quests and Daring Visions" (Kouveliotou et al. in Enduring quests-daring visions (NASA astrophysics in the next three decades), 2014, arXiv:1401.3741), in the areas of: 1) the Interstellar Medium and Planet Formation, 2) Exoplanets, Astrobiology, and the Solar System, and 3) Galaxies. The *OASIS* science objectives require space-borne observations of galaxies, molecular clouds, protoplanetary disks, and solar system objects utilizing a telescope with a collecting area that is only achievable by large apertures coupled with cryogenic heterodyne receivers. *OASIS* will deploy an innovative 14-meter inflatable reflector that enables >16× the sensitivity and >4× the angular resolution of *Herschel*, and complements the short wavelength capabilities of *James Webb Space Telescope*. The *OASIS* state-of-the-art cryogenic heterodyne receivers will enable high spectral resolution (resolving power $> 10^6$) observations at terahertz (THz) frequencies. These frequencies encompass far-IR transitions of water and its isotopologues, HD, and other molecular species, from 660 to 63 μm that are otherwise obscured by Earth's atmosphere. From observations of the ground state HD line, *OASIS* will directly measure gas mass in a wide variety of astrophysical objects. Over its one-year baseline mission, *OASIS* will find water sources as close as the Moon, to galaxies ∼4 billion light years away. This paper reviews the solar system science achievable and planned with *OASIS*.

Keywords Solar system science · Planetary atmospheres · Comets · Active icy moons · THz spectroscopy · Heterodyne spectral resolution · Flight mission concept

The Orbiting Astronomical Satellite for Investigating Stellar Systems (OASIS)
Edited by Hans Bloemen

Extended author information available on the last page of the article

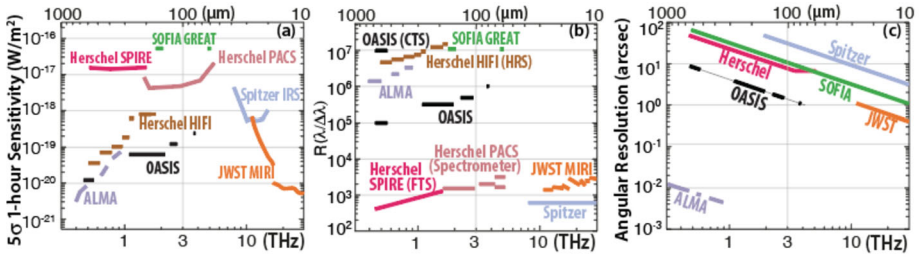

Fig. 1 Spectral line sensitivity (**a**), resolving power (**b**), and angular resolution (**c**) comparisons between *OASIS* and other far-infrared telescopes. *OASIS* provides (**a**) spectral line sensitivity comparable to that of *JWST* and ALMA, and one or more orders-of-magnitude better than *Herschel* or *SOFIA*, (**b**) spectral resolving power comparable to the best available with *SOFIA* and ALMA, and (previously) with *Herschel*, and (**c**) nearly an order-of-magnitude improvement in angular resolution relative to past and present far-infrared telescopes. Lower values of sensitivity and angular resolution are better; higher values of resolving power are better

1 Strategic Motivation

While water is crucial for the emergence of life as we know it, there remain many unresolved questions such as: *Where does Earth's water come from?* To make significant progress towards resolving this question requires space-borne observations of planets, moons, and comets within our solar system, targeting the low energy transitions of water and its isotopologues ($H_2^{16}O$, $H_2^{17}O$, $H_2^{18}O$, and HDO) at submillimeter and far-IR wavelengths. The *Orbiting Astronomical Satellite Investigating Stellar Systems (OASIS)* observatory, an Astrophysics MIDEX-class mission concept, is a 14-m class space observatory that will perform high spectral resolution observations at submillimeter and far-IR wavelengths with a single purpose: *follow the trail of water from galaxies to protoplanetary disks to our solar system.* Large space observatory apertures using traditional approaches have proven difficult and costly given that instruments operating at long wavelengths suffer from an inherent restriction on angular resolution; the spatial resolution of the telescope in terms of FWHM (Full Width at Half Maximum) is $1.22\lambda/d$, where λ is wavelength and d is the primary mirror's diameter. In order to achieve small angular resolution while simultaneously increasing sensitivity, large primary apertures are *vital*. This is evidenced by the *James Webb Space Telescope* (*JWST*) mission, where the telescope's primary mirror is 6.5-m in diameter, compared to *Herschel* and *Hubble Space Telescope's (HST)* primary mirrors, which are 3.5-m and 2.4-m, respectively. The size of the primary aperture is directly correlated with telescope sensitivity since a larger diameter enables a larger area to collect more photons (see Fig. 1). Larger primary apertures, however, increase the cost, mass, and complexity of the flight mission, which is one reason that *JWST* is a Flagship-class Astrophysics mission costing ~$10B. On the other hand, *OASIS* is revolutionizing the field by not only incorporating a 14-m *inflatable* primary aperture but by doing so within the MIDEX Mission cost cap of $300M. The combination of *OASIS* high spectral resolution with its high sensitivity and large spectral grasp is a game changer for space-borne single dish telescopes operating at submillimeter and far-IR wavelengths.

OASIS comprises four tunable-in-frequency spectral bands: 0.455–0.575 THz (Band 1), 1.1–2.2 THz (Band 2), 2.475–2.875 THz (Band 3), and 4.734–4.745 THz (Band 4). As depicted in Fig. 2, *OASIS* Bands 1–4 cover frequency ranges that are essentially opaque to ground-based telescopes, including ALMA. These spectral intervals are extremely rich

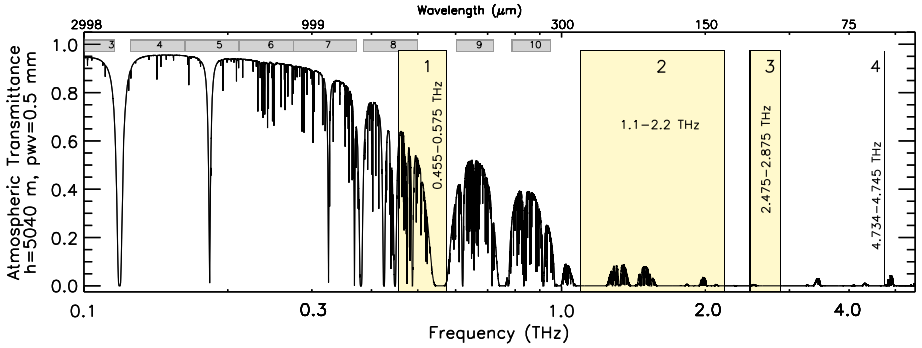

Fig. 2 Simulated terrestrial atmospheric transmission spectrum, corresponding to ALMA's altitude (5040 m) and a relatively low precipitable water vapor of 0.5 mm. The tunable *OASIS* Bands 1, 2, 3, and 4 (numbered yellow rectangles) target wavelengths that are almost completely blocked from the ground, and are highly complementary in frequency to the 10 ALMA bands (ALMA Bands 3 – 10 are indicated by the numbered grey rectangles). The four *OASIS* Bands encompass important transitions of H_2O and its isotopologues as well as many other molecular species, with the Band 3 center capturing the HD $J = 1 \rightarrow 0$ transition

in spectral content, with strong rotational transitions of H_2O isotopologues and numerous other molecules. Figure 2 shows a ground-based transmission spectrum that simulates Earth's atmospheric transmittance for an altitude of 5 km (*i.e.*, for ALMA) and favorable atmospheric water burden (0.5 mm precipitable water vapor [pwv]). This figure reveals that ground-based observations at submillimeter and far-IR wavelengths are severely hampered by Earth's strongly-absorbing atmosphere. The strongest absorbing bands are between 2 mm and ~20 μm (corresponding to frequency intervals of 5 – 500 cm^{-1} or 0.15 – 15 THz), which are partially depicted in Fig. 2. The spectral coverage of the *OASIS* tunable-in-frequency Bands 1 – 4 are illustrated with yellow rectangles, and the ten available ALMA receiver bands are shown by the grey rectangles, positioned in regions of relatively favorable transmittance.

The extreme opacity of Earth's atmosphere in the submillimeter and far-IR is the reason that ALMA has made only very few measurements of HDO and $H_2^{18}O$ (plus few attempts to detect $H_2^{16}O$), and moreover with ALMA, these measurements can be accomplished only under rare observing conditions (very low pwv, see Jensen et al. 2019; Piccialli et al. 2017). This reinforces the need for space-borne platforms with instruments operating in the far-IR and submillimeter spectral regions. As illustrated in Fig. 2, *OASIS* was designed specifically for this purpose: it is optimized to detect the low energy transitions of $H_2^{16}O$, $H_2^{17}O$, $H_2^{18}O$, and HDO over a large spectral range in the far-IR and submillimeter, as well as the $J = 1 \rightarrow 0$ transition of HD at 2.675 THz, all inaccessible to ground-based telescopes.

2 Relevance to Solar System Science

The *OASIS* overarching mission goal is to *Understand how water enables the formation of stellar and planetary systems*. Since the ideal planetary system to investigate the role of water is our own solar system, the *OASIS* solar system science objective will *Characterize the delivery of water to the solar system by investigating its reservoirs*. *OASIS* solar system science links the origin and the chemical and physical evolution of water in protoplanetary systems to the characteristics of water in our own solar system. Comets and asteroids are believed to have delivered water to the early Earth, and each have distinct D/H signatures. *OASIS* will help determine whether or not comets were the principal sources of Earth's water

by measuring the HDO/H_2O ratio in both Jupiter Family Comets (JFCs) and Oort Cloud Comets (OCCs). Moreover, the 16-fold increase in the *OASIS* collecting area with respect to *Herschel* (see Fig. 1) results in a factor of 256 reduction of observing time, enabling the detection of water in more than 20 solar system objects. As expanded on in Sect. 4.1, this will significantly improve upon the accuracy of present-day D/H ratio measurements in both H_2O and H_2 (Fig. 3).

OASIS solar system science is responsive to the 2013 NASA Roadmap (*Enduring Quests Daring Visions: NASA Astrophysics in the Next Three Decades;* Kouveliotou et al. 2014), which advocates completing the reconnaissance of gas giants, terrestrial planets, and Ocean Worlds. *OASIS* will make significant progress towards this since it will measure H_2O abundances in the stratospheres of the Gas Giants in order to determine whether planetary rings, icy moons, interplanetary dust particles, or comet impacts deliver water to these planets. Additionally, *OASIS* will measure the abundance of H_2O and HDO in the atmospheres of Venus and Mars to better understand how their atmospheres have evolved over time. *OASIS* will also measure the H_2O abundance in the torus surrounding Saturn generated by the Ocean World Enceladus, in order to understand how its plume ejecta material (predominately water) has altered the Saturnian environment. Titan, another Ocean World and the largest satellite of Saturn, has a complex atmosphere containing oxygen compounds that may have been delivered from the H_2O torus and, ultimately, from Enceladus. *OASIS* will measure the vertical profile of H_2O in order to constrain its external source. On Titan, methane plays the role that water does on Earth, with its hydrocarbon lakes, tropospheric methane clouds, and methane precipitation. In addition to water, *OASIS* will measure CH_3D and CH_4 in order to determine the inventory of deuterium as well as to better understand the methane cycle on Titan. Gaseous H_2O emission has also been observed from the dwarf planet, Ceres; however, its source and spatial distribution are not known. The high sensitivity of *OASIS* will allow us to determine whether cryo-volcanism or ice sublimation from localized regions is the source of water. Moreover, the regolith of the Moon contains water ice that may sublimate to form an H_2O exosphere, and the density and spatial variation of the exosphere is unknown. The unique vantage point of *OASIS* at the L1 Lagrange point permits high spatial resolution observations of the Moon, including the south polar region, which is a primary focus of human exploration. Thus, *OASIS* will contribute towards both pure science and resource utilization on the Moon, paving the way for future programs like Artemis. This same L1 vantage point will permit detailed observations of the upper atmosphere of Venus. In addition to measuring D/H, *OASIS* will observe numerous sulfur compounds, and it will confirm (or refute) the controversial detection of PH_3.

The solar system measurements will also answer fundamental, high-priority science questions presented in the Astrophysics Decadal Survey (*Pathways to Discoveries in Astronomy and Astrophysics for the 2020s;* National Academies of Sciences and Medicine 2021). *OASIS* solar system science addresses Decadal Questions E-Q2 and E-Q3: *What are the properties of individual planets, and which processes lead to planetary diversity? How do habitable environments arise and evolve within the context of their planetary systems?* To accomplish this, *OASIS* will observe approximately two dozen solar system objects over its 1-year baseline mission. The following sections expand on the justification for conducting highly unique, compelling, and cutting-edge solar system science with *OASIS*.

3 The Need for D/H

Deuterium fractionation is sensitive to extant conditions (most significantly, temperature) during the epoch of solar system formation. As a result, the D/H ratio is a well-established

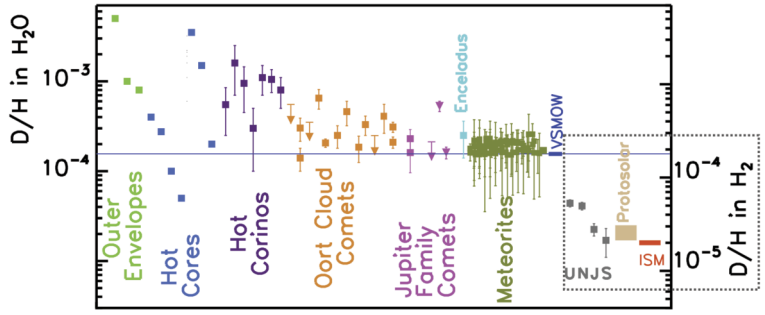

Fig. 3 D/H ratios for various classes of interstellar and solar system objects. The left ordinate reflects the "cometary" notation for the D/H value in water, which is 1/2 the value of HDO/H_2O. This is reflected in the values shown for the star-forming regions (Outer Envelopes, Hot Cores, and Hot Corinos), comets, Enceladus, Earth's oceans (VSMOW), and carbonaceous meteorites. The values of D/H in water demonstrate that this [minor] reservoir of deuterium is highly fractionated, as low temperature chemistry greatly enhances small zero-point energy differences between isotopologues favoring the deuterated species. The right ordinate, and also indicated by the grey dotted rectangle, gives the D/H values in H_2 for the Giant Planets, the ISM, and the protosolar nebula, representing the major reservoir of elemental deuterium. As with water, the D/H ratio in molecular hydrogen is half the measured abundance ratio HD/H_2. The figure shows that interstellar and solar system objects exhibit large intrinsic dispersions that are well above uncertainties associated with individual measurements, which *OASIS* will improve upon substantially (*e.g.*, see Sect. 4.1). *OASIS* will measure the HDO/H_2O abundance ratio in a representative sample of protoplanetary disks and solar system objects, and the HD abundance in the Giants Planets, in which the latter measures the major reservoir of elemental deuterium. Figure adapted from (Hartogh et al. 2011b; Lis et al. 2013; Bockelée-Morvan et al. 2015), with additional inputs from (Jensen et al. 2019; Biver et al. 2016; Bockelée-Morvan et al. 2012; Villanueva et al. 2009; Gibb et al. 2016; Paganini et al. 2017; Lis et al. 2019; Biver et al. 2022; Coutens et al. 2012, 2013, 2014; Persson et al. 2014; Wang et al. 2012; Emprechtinger et al. 2013; van der Tak et al. 2006; Helmich et al. 1996; van Dishoeck et al. 2021; Bonal et al. 2013; Yang et al. 2013; Jacquet and Robert 2013)

diagnostic for measuring isotopic fractionation in the early solar system. The variation in measured D/H ratios for various solar system objects provides important clues to the formation conditions at different locations in the nascent solar system. Of particular interest is how the D/H ratio varies in water. The formation process of water involving chemical reactions on interstellar ice grains favors heavier water isotopologues (Watson 1974; Brown and Millar 1989). The D/H ratios in the water measured for molecular clouds and protostellar envelopes are approximately 10^{-2} and 10^{-3}, respectively (Ceccarelli et al. 2005; Butner et al. 2007). As demonstrated in Fig. 3, this is an enrichment of 2 to 3 orders of magnitude over the D/H ratio of protosolar hydrogen (2.1×10^{-5}; Lellouch et al. 2001) and in the local interstellar medium (1.6×10^{-5}; Linsky et al. 2006). These values may be considered to bracket the D/H ratios of water in our solar system, allowing for the possibility of isotopic exchange between water and hydrogen.

Figure 3 shows D/H ratios in water for comets, Enceladus, Earth's oceans (represented by Vienna Standard Mean Ocean Water, or "VSMOW"), carbonaceous meteorites, and star forming regions, and in molecular hydrogen for the Giant Planets, the ISM, and the protosolar nebula. However, care must be taken when comparing the D/H ratio in hydrogen and water: the D/H ratio in hydrogen is mainly determined by the Big Bang primordial nucleosynthesis combined with stellar astration (Peebles 1966; Epstein et al. 1976; Cyburt et al. 2016), whereas the formation process for water requires chemical reactions on the surfaces of interstellar ice grains at very low temperatures (*e.g.*, ∼10 K), with highly efficient formation of deuterated water being demonstrated experimentally (Dulieu et al. 2010). In spite of

this distinction between hydrogen and water, the range of D/H observed within each class of object in Fig. 3 suggests a commensurate range of formative conditions.

Given that D/H ratios in water measured for molecular clouds and protostellar envelopes are respectively about 10 to 100 times higher than VSMOW (Ceccarelli et al. 2005; Butner et al. 2007), the question that arises is: *Why is D/H in VSMOW depleted compared with that in molecular clouds and in protostellar envelopes (representing at least partially ISM material)?* Is this depletion representative of a chemical memory from a previous evolutionary phase? If so, the relevant processes for this chemical evolution remain unknown. *OASIS* will make significant progress towards addressing these questions, through measurement of the HDO/H_2O abundance ratio in a representative sample of protoplanetary disks and solar system objects. This will establish – at an unprecedented level – the evolution of HDO/H_2O from the dark molecular cloud value ($\sim 10^{-2}$), to Hot Cores and Hot Corinos ($\sim 2\times 10^{-3}$), to the [unknown] value of mature protoplanetary disks, to values in the present-day solar system.

Obtaining the most robust value for cometary D/H requires measuring the H_2O production rate as near-simultaneously as possible with multiple lines of HDO. This is difficult because as discussed, the most favorable (*i.e.*, strongest) rotational and vibrational lines of H_2O are not observable from the ground, and for lines that are observable, H_2O and HDO are not encompassed simultaneously by any existing ground-based spectrometers. As a result, most estimates rely on the detection of only a single HDO line that was not measured simultaneously with H_2O (or, in the near-IR, of multiple HDO lines individually having insufficient signal-to-noise ratio; see Villanueva et al. 2009; Gibb et al. 2016; Paganini et al. 2017). Moreover, differing values can be retrieved even for a given comet owing to the use of different techniques by different investigators (as seen for two OCCs and for one JFC in Fig. 3). For this reason, a self-consistent dataset has been obtained for only two comets, using the Heterodyne Instrument for the Far-Infrared (HIFI) spectrometer on *Herschel*: the HDO 509 GHz line was detected quasi-simultaneously with the $H_2^{18}O$ 547 GHz and the $H_2^{16}O$ 557 GHz lines in one JFC (103P/Hartley 2; Hartogh et al. 2011b) and in one OCC (C/2009 P1 Garradd; Bockelée-Morvan et al. 2012). With SOFIA, only a tentative [3.1σ] detection of the HDO 509 GHz line was achieved, albeit near-simultaneously with the $H_2^{18}O$ 547 GHz line, in JFC 46P/Wirtanen (Lis et al. 2019). This paucity of D/H measurements in cometary water will be overcome with *OASIS*.

3.1 The Formation of Water in the Solar System

Figure 4 illustrates how the origin of water in our solar system may be traced through measurement of the water D/H ratio. This figure also sheds some light on the question posed above regarding its relative depletion in VSMOW. In the inner region of the disk (near the Sun) under pressures of 10 μbar to 1 mbar, and temperatures between 600 K and 1300 K (*e.g.*, compare to Fig. 1 in Yang et al. 2013), within a few hundred years, gaseous water equilibrates with hydrogen, which is at least 4 orders of magnitude more abundant. This means that the D/H ratio in water, which was initially highly enriched, will be de-fractionated to its value in molecular hydrogen. With increasing heliocentric distance, temperature and density decrease, as does the efficiency of the isotopic exchange, which stops at an intermediate distance from the Sun where water is still present in gaseous form; this distance is indicated by the "equilibration line" in Fig. 4.

Vertical mixing between the disk mid-plane and photosphere is very important. The key process is mixing of ice grains to the surface of the disk where photodesorption and photochemistry produce atomic oxygen. This is then transported downwards, where chemistry

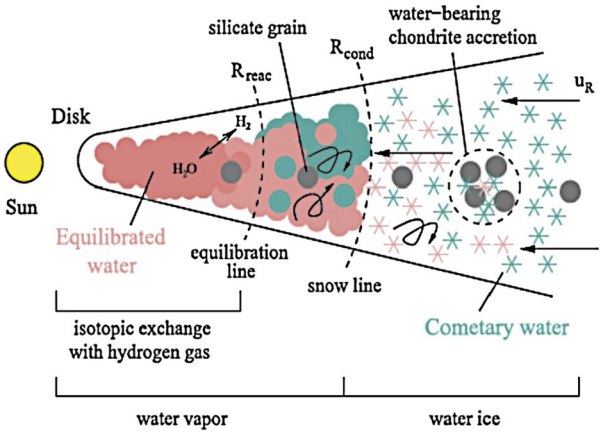

Fig. 4 Illustration of the formation of a D/H gradient with heliocentric distance. Arrows symbolize motions of gas (reprinted from Jacquet and Robert 2013). *OASIS* will permit probing conditions across this gradient

reforms H_2O and HDO on ice grain surfaces but with much reduced fractionation (see for example Furuya et al. 2013). This represents the region in the solar nebula where chemistry can affect the HDO/H_2O ratio out to some 50 AU from the young Sun on a timescale of 1 Myr. Additionally, since the gas and dust are much warmer than the cold interstellar clouds, the deuterium fractionation of H_2O will be much smaller. The net result will be a radial gradient in the average HDO/H_2O ratio (increasing with distance from the Sun) and a temporal evolution set by the strength of mixing and chemical timescales involved (both of which decrease with time). This process is reflected in Jupiter and Saturn's atmospheric HD/H_2 ratios (within existing uncertainties), which reflect the protosolar nebula value (Lellouch et al. 2001; Pierel et al. 2017), while the HD/H_2 ratios in the Ice Giants (Uranus and Neptune) are more fractionated (Feuchtgruber et al. 2013), reflecting the high ice mass and the importance of these equilibration reactions (Furuya et al. 2013).

While pebbles drifting inward from the cold outer ranges of the solar nebula will contribute relatively pristine presolar ice material with high HDO/H_2O ratios to the inner solar system regions, there are many processes that affect the HDO/H_2O ratio. These include gas phase chemistry in the warm inner regions of the solar nebula coupled with turbulent mixing outwards, vertical mixing of material coupled with photodesorption, photo-dissociation, and grain surface chemistry, drifting of pebbles with preserved molecular cloud material inwards, and sequestering of material into planetesimals and cometesimals. Although the relative importance of these processes is currently unknown, we do know they will cause a radial and temporal variation in the HDO/H_2O ratio. *OASIS*, with its dedicated solar system and protoplanetary disk observing program to determine HDO/H_2O ratios, is optimized to study these processes in detail.

4 Overview of *OASIS* Solar System Science

4.1 Comets

Since comets are generally considered the most primitive bodies in the solar system, comprised of icy planetesimals left over from planet formation, they are ideal for constraining the origin and thermal evolution of water in the solar nebula. As with other classes of objects represented in Fig. 3, the D/H ratios in water for comets show an intrinsic dispersion that is larger than the uncertainties associated with the individual measurements, which for comets

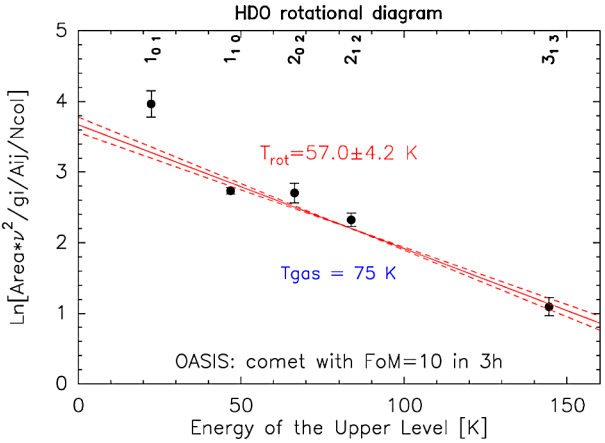

Fig. 5 Rotational diagram based on a full non-LTE model simulation for *OASIS* observations targeting cometary HDO lines at 0.465, 0.509, 0.491, 1.278 and 1.625 THz (having upper levels 1_{01}, 1_{10}, 2_{02}, 2_{12}, and 3_{13}, respectively, as labeled). Note these lines have energies bracketing the gas temperature. *OASIS* will measure multiple lines of HDO to derive gas temperatures in comets, and the small beam size (even in Band 1) will reduce uncertainties in gas temperature, although several lines are still needed due to significant departure from LTE

span approximately 1 to 3 times that of VSMOW. Given that differences in measurements also exist for individual comets suggests that systematic uncertainties could be significant, perhaps resulting from independent measurements (and retrievals) by different observers. A significant systematic difference in HDO/H_2O between dynamical classes (JFCs versus OCCs) may not be the driving factor for these observed differences in the D/H values in water. Similarly, the large spread of values for D/H in water could suggest that the location where comets formed in the early solar system may not be the key parameter in determining the D/H value in water, although as mentioned uncertainties due to the technique used could also play a role. Rather, the water D/H value may be controlled by both the radial location where a given comet was formed and when its constituent ices became insulated from the vertical mixing between the disk mid-plane and photosphere that drives gas-phase D/H exchange (see discussion above in Sect. 3).

To date, there are measurements of cometary HDO at wavelengths ranging from the UV to sub-millimeter; however, these are relatively few in number. HDO was detected through its vibrational band around 2720 cm^{-1} (Villanueva et al. 2009; Gibb et al. 2016; Paganini et al. 2017), through its rotational lines at 0.241 THz (Biver et al. 2016) and 0.465 THz (Bockelée-Morvan et al. 2015; Meier et al. 1998), and indirectly via detection of OD (Hutsemékers et al. 2008) or D-Lyman-α (with HST; Weaver et al. 2008). The HDO 0.509 THz line was targeted once from the ground, but was not detected (Biver et al. 2006). A different instrument was used for each HDO measurement, and with the exception of *Herschel* (see below), HDO was not observed simultaneously with other isotopes of water, either in the IR or sub-mm regimes. HDO and H_2O were measured in situ (via mass spectrometry), but for only two comets (1P/Halley and 67P/Churyumov-Gerasimenko), during the Giotto and Rosetta space missions, respectively (Eberhardt et al. 1987; Altwegg et al. 2015). As a result, D/H ratios in water have been reported in only 16 comets, 4 of which are upper limits and 7 of which were obtained from the ground (Fig. 3).

As discussed in Sect. 1, due to atmospheric opacity, direct ground-based observations of $H_2^{16}O$ line emission in the near-IR are restricted to weaker (non-fundamental, or "hot") bands in the ~2.8-3.0 μm and 4.6-5.0 μm spectral regions (*e.g.*, see Dello Russo et al. 2016; Mumma and Charnley 2011, and references therein). Also owing to atmospheric opacity, neither has cometary $H_2^{16}O$ nor $H_2^{18}O$ been detected in the radio from the ground (and accessible lines are too weak).

Figure 5 shows a rotational diagram of HDO for a simulated observation with *OASIS*: HDO is not in LTE and it is essential to observe several transitions to retrieve a represen-

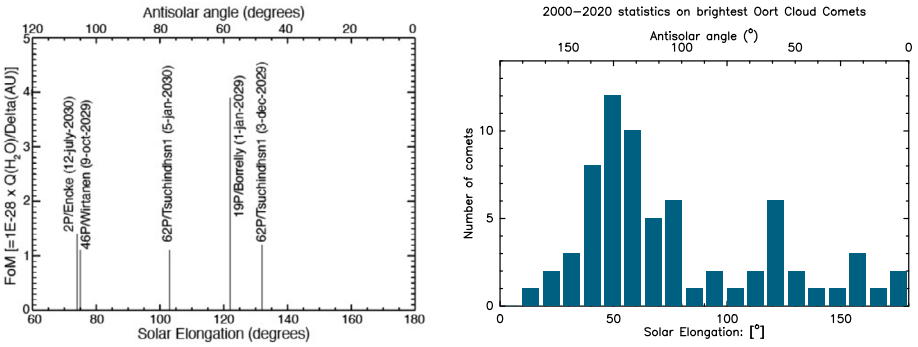

Fig. 6 Left: Observing circumstances for 4 JFCs during the *OASIS* 1-year baseline mission (2029-2030), showing expected radio Figure-of-Merit (FoM) versus solar elongation angle. Right: 20-year histogram of OCC apparitions representing the brightest comets, 80% of which had solar elongation >45°, and thus would easily be observable by *OASIS*. We expect 5 – 6 sufficiently bright OCCs to become available to *OASIS* during any given 1-year period, based on these statistics

tative gas rotational temperature. *OASIS* will observe up to 5 different lines of HDO, with near simultaneous observations of $H_2^{16}O$ and its $H_2^{18}O$ and $H_2^{17}O$ isotopologues – these last two are needed to address opacity issues in $H_2^{16}O$ lines in more productive comets – to establish precise production rates for both HDO and H_2O, and hence D/H ratios. *OASIS* will therefore not only add to the number of comets measured, but most significantly will greatly increase the number of accessible water isotopologue lines that are totally blocked from the ground. This will also provide a unique set of measurements using a single observing platform and set of instruments, thereby greatly reducing sources of systematic error associated with previous work as represented in Fig. 3.

In the *OASIS* 1-year baseline mission, we estimate 6 – 8 comets will be observed. Figure 6 (left panel) identifies 4 JFCs having favorable apparitions, in which radio Figure-of-Merit (an estimate of spectral line brightness) is shown versus solar elongation angle; *OASIS* is designed for targets >45° from the Sun. We also estimate 3 – 4 OCCs becoming available for study (Fig. 6, right) based on discovery statistics from NEO survey programs over the past two decades that discovered long-period comets as a by-product; these are currently dominated by the Catalina and Pan-STARRS surveys (*e.g.*, Morgan et al. 2014).

Additionally, analysis of debiased data from the NEOWISE prime-mission survey (Mainzer et al. 2014) suggest that approximately 7 long-period comets (OCCs) that are one km or larger in diameter come within 1.5 AU of the Sun each year (Bauer et al. 2017). Given the high sensitivity of *OASIS*, in our estimate of 3 – 4 OCCs, we expect one or more targets that are sufficiently productive to be characterized even when not at maximum brightness, but when more favorably placed for long duration (multiple-hour) observations with *OASIS* (*i.e.*, at smaller antisolar angles).

Through its uniform set of measurements of HDO/H_2O, *OASIS* will therefore greatly improve the accuracy over existing measurements of D/H in comets by establishing, in a systematically consistent manner, its value in comets fed from the two principal solar system reservoirs, the scattered Kuiper disk (principal source of JFCs) and Oort cloud (principal source of OCCs). Figure 7 shows a simulation of a typical comet with *OASIS* Bands 1, 2, and 3. Through comparison with D/H in Earth's oceans (VSMOW; see Fig. 3), cometary D/H measurements constrain the role of comets in delivering water to the young Earth, as well as to other planets. However, as discussed above (see Fig. 2), measurement of water and its

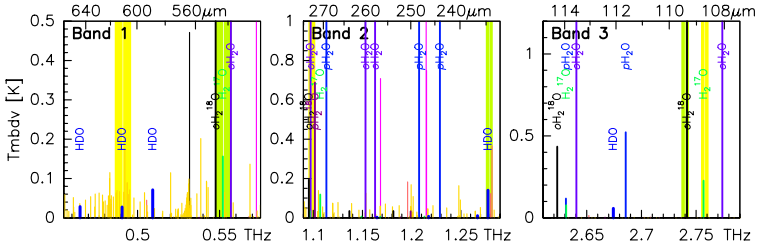

Fig. 7 *OASIS* simulated spectrum of a typical comet observed in Bands 1 (left), 2 (middle), and 3 (right). The water isotopes are identified and indicated by the blue lines. Yellow and green rectangles show examples of simultaneously encompassed (tunable) frequencies combined in Bands 1 – 3 (yellow: 0.491, 1.099, and 2.757 THz [610.6, 272.8, and 108.7 μm] with one setting; green: 0.552, 1.279, and 2.742 THz [543.1, 234.4, and 109.3 μm] with a second setting), demonstrating that *OASIS* will measure HDO, $H_2^{16}O$, $H_2^{18}O$, and $H_2^{17}O$ simultaneously

isotopologues from ground-based observations is extremely challenging due to severe extinction by water in Earth's troposphere. With relatively few tuning changes over the course of a comet observing session with *OASIS*, the strongest transitions of HDO, $H_2^{16}O$, $H_2^{17}O$, and $H_2^{18}O$ will be measured, thereby establishing highly precise isotopic ratios. Additional molecular species will further constrain the gas temperature in the coma, most notably a suite of CH_3OH lines around 0.490 THz.

4.2 Giant Planetary Systems

4.2.1 Enceladus' Water Torus

Enceladus is a fascinating small moon of Saturn that is a prime target for investigating the habitability of Ocean Worlds; it may possibly harbor the conditions for the emergence of life. Ocean Worlds like Enceladus, Europa, Titan, and possibly Ganymede, Callisto, and Triton, are active icy moons orbiting planets that reside far outside the classical "Habitable Zone." Instead, these moons are located in the cold outer solar system, where they are expected to be inactive frozen icy worlds. One of the big discoveries stemming from the *Cassini* 13-year mission in the Saturn system was that Enceladus contained a subsurface liquid water reservoir, which expels hundreds of kilograms of water vapor every second into space through four 2-km wide cracks near its S. polar region (Hansen et al. 2006; Porco et al. 2006; Waite et al. 2006). This small but mighty moon is responsible for both of Saturn's tenuous E-ring, as well as the diffuse cloud of water – a torus – around Saturn that extends vertically 10s of thousands of km (see Hartogh et al. 2011a, for more details). Both Saturn's E-ring and torus are visible (and indicated) in Fig. 8.

The *Herschel* HIFI instrument discovered the Enceladus water torus by measuring the spatial variation of H_2O at 1.670 THz (Hartogh et al. 2011a). Water was observed in absorption against the disk of Saturn and in emission away from Saturn. The spatial resolution of *Herschel* at 1.670 THz was 12.6″. *OASIS* will measure this same transition with a spatial resolution of 3.2″ and with higher sensitivity. *OASIS* will also measure multiple lines of H_2O to derive the gas temperature in the torus. We will expand on the *Herschel* science by providing a higher spatial resolution map of the torus and by targeting transitions of HDO, $H_2^{17}O$, and $H_2^{18}O$ to derive isotopic ratios. Since water originates from a subsurface liquid reservoir, these measurements will provide a rare opportunity to probe conditions in the interior of Enceladus. Due to the small angular size of Enceladus (0.07″), observing it directly

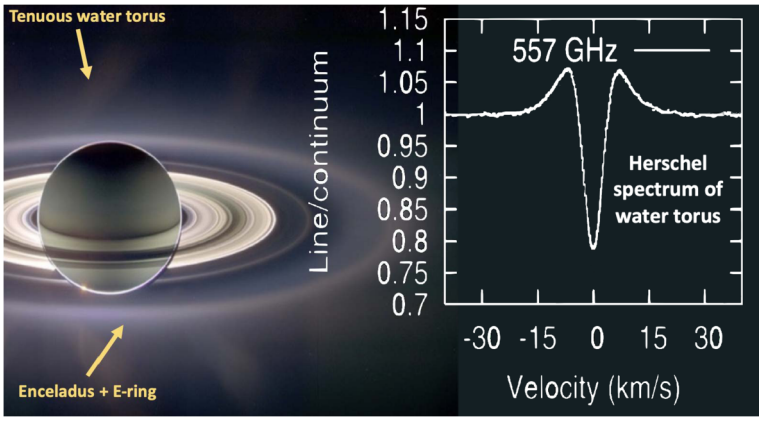

Fig. 8 *OASIS* will measure the spatial variation of the tenuous water torus around Saturn generated by its icy moon Enceladus. Water ice is largely confined to the E-ring in Saturn's equatorial plane, but gaseous water extends tens of thousands of kilometers above the ring plane, as discovered by *Herschel*/HIFI (water spectrum on right hand side reprinted from Hartogh et al. 2011a). *OASIS* will observe low excitation energy water lines emitting from the Giant Planetary Systems to determine the external water delivery sources. This will significantly improve upon the *Herschel*/HIFI observations. Saturn Image Credit: NASA/JPL/Space Science Institute

with *OASIS* will be extremely challenging since we will suffer from severe beam dilution, even with the small beam size at the high frequency end of Band 4 (1.1″). However, in lieu of a direct detection from the plumes themselves, the large spatial expanse of Enceladus' torus offers a unique opportunity to measure the water isotopic ratios for an Ocean World, which are greatly needed to constrain the origin of its water, as well as how it has evolved over time.

To date, there has only been one isotopic measurement of water in Enceladus' plume itself. *Cassini* INMS obtained a D/H value of $2.9^{+1.5}_{-0.7} \times 10^{-4}$ (Waite et al. 2009), an enhancement of 1.9 times that in Earth's oceans (see Fig. 3). Until another planetary flight mission is sent back to the Saturn System to study Enceladus, the *OASIS* high sensitivity is capable of building on both the *Cassini* and *Herschel* science discoveries.

4.2.2 Giant Planets' HD Abundance

The bulk reservoir for deuterium in the Giant Planets is in the form of HD. And, since there are no known post-Big Bang processes to create deuterium, the deuterium abundances in the Giant Planet atmospheres – measured today – are taken to reflect their primordial value. Accurate measurements of D/H in the Giant Planets are needed to constrain models of their origin, but it is difficult to measure HD since this can only be accomplished from space-borne platforms (and airborne observatories such as SOFIA). *OASIS* will measure HD/H_2 in all of the Giant Planets, thereby providing the bulk D/H ratio. *OASIS* will also measure stratospheric H_2O in the Giant Planets (see Sect. 4.2.5), but not HDO; thus, it will not be possible to measure D/H in H_2O for the Giant Planets. These planets have $\sim$1 ppb H_2O in their stratospheres due to external sources (see discussion in Sect. 4.2.5). The expected abundance of HDO is $<$1 ppt and, thus, below the *OASIS* detection limit. Larger amounts of H_2O are present at pressures greater than 5 bars in the Giant Planets; however, sub-millimeter observations do not probe deep enough to detect tropospheric H_2O nor HDO.

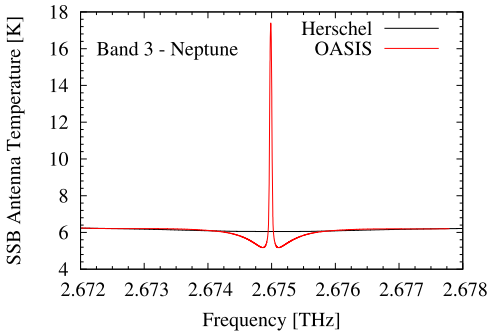

Fig. 9 *OASIS* will use its high spectral resolution to improve the accuracy of D/H in the outer planets. *Herschel*/PACS detected a weak HD absorption line on Neptune at a resolving power of 950 (Feuchtgruber et al. 2013). *OASIS* (red curve) will measure this same feature at more than 100 times this resolution, revealing both stratospheric emission and tropospheric absorption – OASIS will resolve the narrow central emission line that dominates the line profile, and will retrieve significantly more accurate D/H. If *OASIS* only had the resolving power of PACS (black line), it would miss this central emission peak. Resolving the full line shape is critical to determining accurate D/H ratios. (SSB stands for single side band)

In the core accretion scenario for Giant Planet formation (Pollack et al. 1996), highly D-enriched primordial ices formed the planet massive cores onto which the surrounding protosolar H_2 gas collapsed. The resulting HD abundance then results from the ice-to-rock ratio in the core, the core-to-atmosphere mass ratio, and equilibration between the two reservoirs. For instance, the massive H_2-dominated atmosphere of Jupiter surpasses by far the mass of its putative core, and D/H in Jupiter is therefore thought to reflect the protosolar value (Lellouch et al. 2001, see Fig. 3). For Saturn, however, the measured D/H in hydrogen is smaller than in Jupiter (Pierel et al. 2017), which is unexpected if ice played a role since higher D/H in hydrogen should be expected (as it is the case for the Ice Giants) or perhaps, the ice was equilibrated and transported from the inner to the outer solar system. For the Ice Giants, the D/H is ∼2 times higher than the Gas Giants due to a much thinner outer envelope of H_2, thereby increasing the weight of the ice-originating D in the final abundance of HD after equilibration (Feuchtgruber et al. 2013). The 4–10 times lower D/H compared with comets remains unexplained. There may be more rocky than icy material in the interior of Uranus and Neptune than expected from formation models (Feuchtgruber et al. 2013). There are various scenarios that could constrain the precise formation position of the Ice Giants with respect to the various snowlines (*e.g.*, Ali-Dib et al. 2014; Mousis et al. 2020). However, error bars on existing measurements of D/H in all four outer planets are still large and need to be reduced in order to answer the following questions: *Is Saturn's D/H also protosolar? If its D/H is lower than the protosolar value, as indicated by its nominal value measured by ISO and by Cassini/CIRS, what is the mechanism causing this depletion? What is the reason for the intermediate D/H in Ice Giants compared with the protosolar value and comet values? OASIS* will be able to measure HD in all four Giant Planets, which will significantly improve upon existing HD measurements from *ISO*, *Herschel*, and *Cassini*/CIRS. *OASIS* will also measure D/H in methane (CH_3D/CH_4) in the Ice Giants to further investigate fractionation of deuterium at low temperatures.

The *Herschel* Photodetector Array Camera and Spectrometer (PACS) did not have sufficient spectral resolution to resolve the narrow HD emission line core originating from the Giant Planet stratospheres. *ISO* and CIRS also lacked the spectral resolution to separate stratospheric emission from tropospheric absorption, thus limiting the accuracy in deriv-

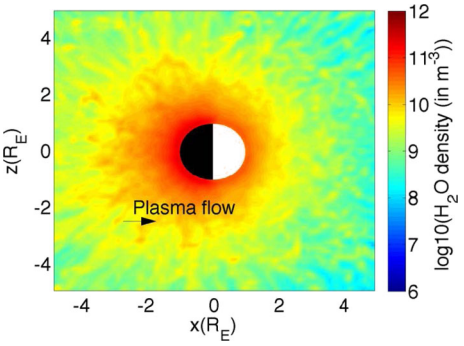

Fig. 10 OASIS will test models of the water atmospheres of Europa (shown here, Plainaki et al. 2018), Ganymede, and Callisto by measuring both leading and trailing hemispheres of these active icy moons

ing HD/H_2. *OASIS* however, will easily resolve the narrow emission line core, enabling the derivation of D/H in the stratospheres of the Giant Planets; this is depicted for Neptune in Fig. 9. Although HD is expected to be well mixed, *OASIS* will be able to test this assumption. *OASIS* will measure independently D/H in the upper troposphere and in the stratosphere and, thus, separate both contributions to the spectrum, similar to what was performed for CO and the deep O/H ratio in Neptune (Luszcz-Cook and de Pater 2013; Cavalié et al. 2017). We will thus better constrain the deep tropospheric D/H ratio, which is needed to constrain formation processes. However, the derivation of D/H from the emission core of HD in the Giant Planets requires knowledge of the stratospheric temperature profile. *OASIS* will measure CO and CH_4 in Band 2 (1.1 to 2.2 THz) to obtain the temperature profile for the stratosphere. *OASIS* also has broad-band continuum channels in each of its 4 bands. These will be used to derive the temperature of the upper troposphere, which is needed to interpret the absorption component of the HD line. *OASIS* will also have improved spatial resolution (2.0″ at 2.675 THz) with respect to *Herschel* (∼10″) and *ISO* (∼20″).

4.2.3 Galilean Moons' Water Atmospheres

The Hubble Space Telescope detected transient H_2O plumes at Europa in the UV, which were tentatively confirmed with ground-based facilities (Paganini et al. 2020) and from a reanalysis of Galileo data (Jia et al. 2018). Based on the water vapor abundance reported by Paganini et al. (2020), had the *Herschel* HIFI team been given the observing time on Europa, the HIFI instrument would have easily detected its H_2O plumes. With the *OASIS* 10-fold enhanced capabilities over that of *Herschel*, *OASIS* will be able to confirm the presence of Europa's transient H_2O plumes, and the corresponding water abundance. Investigating Europa's plume composition with the large spectral coverage and high sensitivity of *OASIS* will provide direct access to the composition of the internal ocean. *OASIS* measurements will precede and so will provide guidance for the arrival of Europa Clipper in 2030.

Herschel did observe tenuous and spatially variable H_2O atmospheres at Ganymede and Callisto (Hartogh 2022). The process responsible for maintaining these atmospheres, whether it is sputtering, sublimation, hydrothermal activity, or interacting with the icy dust environment of Jupiter, remains unknown. Models have predicted the amount of water vapor and its distribution resulting from sputtering, radiolysis, and sublimation (*e.g.*, Shematovich et al. 2005; Plainaki et al. 2018) for Europa, (Marconi 2007) for Ganymede, and (Liang et al. 2005) for Callisto. For example, in the case of Europa (Fig. 10), a total mass of its water atmosphere was predicted to be ∼20–100 metric tons, substantially lower than predicted for Ganymede and Callisto, and too low to be detected from ground-based observatories or

HST. Transient events, or plume activity, corresponding to about 2,000 tons of total water with a detection limit of 500 tons have been reported (Roth et al. 2014; Paganini et al. 2020). OASIS' Band 2 observations are between 2–3 orders of magnitude more sensitive, *i.e.*, detection limits of ∼1 ton are expected for an integration time of 1 hour in Band 2. Based on the predictions of the models cited above, *OASIS* will detect the water atmosphere of the three moons without the need for transient events/plumes. *OASIS* will conduct repeated observations of H_2O lines at Ganymede, Callisto, and Europa as a function of their orbital position (*e.g.*, leading vs. trailing), and this will help to constrain the relative role played by these processes, as well as set the stage for the ESA JUpiter ICy moons Explorer (JUICE) and NASA Europa Clipper missions (Ilyushin and Hartogh 2020; Grasset et al. 2013; Hartogh and Ilyushin 2016; Howell and Pappalardo 2020).

4.2.4 Triton

Voyager 2 detected plumes rising from the surface of Neptune's largest moon, Triton (Soderblom et al. 1990; Yelle et al. 1991). These are thought to be composed of N_2 with entrained condensates. Triton's surface temperature is 38 K, making it unlikely to have gaseous H_2O. However, if Triton has cracks in its ice, analogous to those on Enceladus, warmer temperatures may be possible. *OASIS* will search for H_2O outgassing from the surface of Triton. Although unlikely, a detection of H_2O would radically change our concept of activity on icy moons in the outer solar system, especially at Neptune's distance of 30 AU from the Sun. The recent Planetary Science Decadal Survey (National Academies of Sciences and Medicine 2022) ranked a Flagship mission to an ice giant system as a top priority for the next decade. Even though both ice giant systems have superlative scientific merit, the decadal committee ended up favoring the Uranus Orbiter and Probe Flagship mission over the Neptune Odyssey Flagship mission. Neptune was also not selected as a mission candidate for New Frontiers 6 or 7, so the *OASIS* observations are even more critical for remote sensing measurements of the Neptune System.

4.2.5 External Sources of Water

Stratospheric water on Jupiter was first detected from the Kuiper Airborne Observatory immediately following the impact of comet Shoemaker-Levy 9 (SL9; Bjoraker et al. 1996). Shortly thereafter, H_2O was observed in emission by *ISO* at millibar levels in the stratospheres of all four Giant Planets and Titan (Feuchtgruber et al. 1997; Coustenis et al. 1998). For the Giant Planets, trace amounts of water were observed in emission at millibar levels in these atmospheres. Water originating from the deep atmosphere is frozen out at the tropopause (100 mbar) where temperatures are less than 120 K; thus, the presence of H_2O in their stratospheres implies an external source.

Water vapor in Titan's stratosphere is also trace, with *Cassini* CIRS far-IR nadir and limb sounding measurements revealing a volume mixing ratio of (on average) ∼0.3 ppb in Titan's stratosphere (Cottini et al. 2012). As with the Giant Planets, the source of water in Titan's stratosphere is externally delivered, given that water freezes out in Titan's lower stratosphere as a result of vapor condensation processes. Even more so, a positive vertical gradient was derived from CIRS far-IR (Cottini et al. 2012) and *Herschel* (Moreno et al. 2012) observations, indicating a source above at higher altitudes and a sink below at lower stratospheric altitudes. This result further reinforces the idea that water is externally delivered to Titan.

OASIS will constrain the role of icy moons in the delivery of species like H_2O to the upper atmospheres of the Giant Planets and Titan. *OASIS* will be able to assess the relative

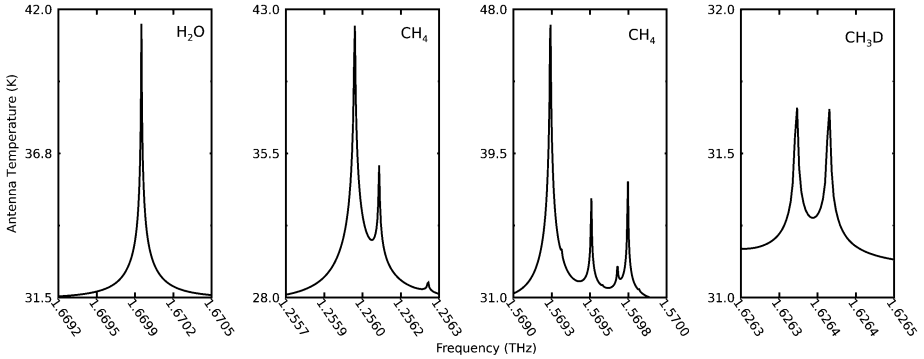

Fig. 11 Radiative transfer simulations of the disk-center stratospheric H_2O, CH_4, and CH_3D emission from Titan at 1.670 THz, 1.256 THz, 1.570 THz, and 1.626 THz, respectively. The *OASIS* beam size is ∼3-4″ at these frequencies so Titan's disk (0.8″) is spatially unresolved. Spectral resolution is 3.5 MHz

contributions of interplanetary dust, icy rings and moons, and large comet impacts by measuring the variation with latitude of H_2O transitions at 1.670 and 4.745 THz, and at spatial resolutions of 3.2 and 1.1″, respectively. The former transition is 100 times stronger than the latter at 150 K, while the 4.745 THz line offers better spatial resolution. The smaller beam size (1.1″) will roughly match the angular size of Titan (0.8″). The use of two lines with different strengths will yield improved vertical profiles of H_2O in the stratospheres of these objects, which will further constrain its source. In addition, *OASIS* will also measure the $H_2^{18}O$ transition at 1.656 THz, thereby providing important isotopic information about the impactors.

In addition to H_2O, *OASIS* will also measure CH_4 and CH_3D in Titan's stratosphere. While measuring the vertical profile of water in Titan's atmosphere will help to constrain its external source, measuring the vertical profiles of both CH_4 and CH_3D is important as well, given that on Titan, CH_4 plays the role that water does on Earth, evidenced by its hydrocarbon lakes, tropospheric CH_4 clouds, and CH_4 rain (*e.g.*, see (Griffith et al. 2005; Porco et al. 2005; Turtle et al. 2009, 2011; Anderson et al. 2014)]. *OASIS* will measure CH_4 and CH_3D above Titan's cold trap, well above all the tropospheric CH_4 weather cycles. Figure 11 shows a forward radiative transfer model simulation of H_2O, CH_4, and CH_3D emission on Titan at 1.670 THz (H_2O), 1.256 and 1.570 THz (CH_4), and 1.626 THz (CH_3D).

High spatial resolution will permit *OASIS* to distinguish between possible external sources of water. Interplanetary dust particles (IDP) should impact the Giant Planets from all directions, while local sources such as rings and icy moons would preferentially deliver water to the Equator. For instance, *Herschel*/PACS measurements of an H_2O enhancement between 25°N and 25°S on Saturn favor Enceladus and its H_2O torus as the dominant source (Cavalié et al. 2019). *Cassini*/CIRS measurements of H_2O at the poles of Saturn indicate that there is a smaller component due to IDP (Bjoraker 2022). *Cassini* in situ observations revealed an infall of gases including H_2O from Saturn's D-ring confined to within 8° of the Equator (Waite et al. 2018). *OASIS* measurements of H_2O at the North and South Poles of Jupiter and at the South Pole of Saturn[1] will reveal the component due to IDP. A detection of enhanced H_2O over a narrow latitude range at the Equator would favor a ring source and an enhancement over a wider range of latitudes would support delivery from a torus. Higher

[1] Saturn's North Pole will be in polar night and thus not observable during the *OASIS* 1-year baseline mission.

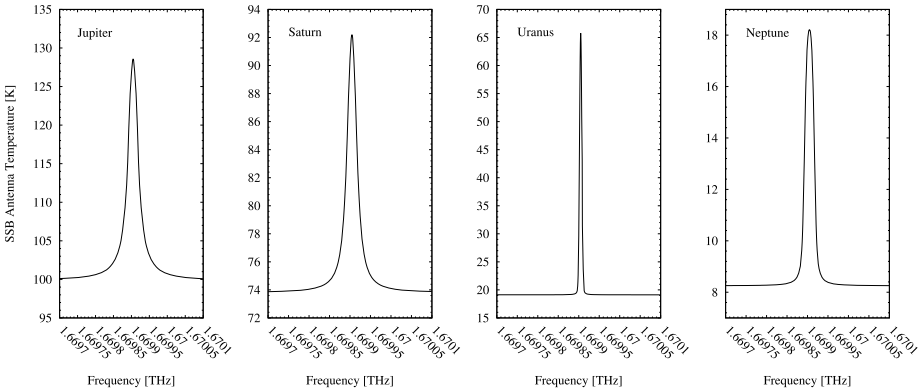

Fig. 12 Simulations of the disk-center stratospheric H_2O emission at 1.670 THz (Band 2) for Jupiter, Saturn, Uranus, and Neptune. SSB stands for Single Side Band

sensitivity and a large improvement in spatial resolution (1.1-3.2″ vs. 9.4″ for PACS) will allow *OASIS* to refine and extend these pioneering measurements.

Figure 12 shows synthetic spectra of H_2O emission at 1.670 THz on Jupiter, Saturn, Uranus, and Neptune. Spectrally resolved line profiles at 1.670 THz provide information on the vertical profile of H_2O in the stratosphere, and also constrain the external source of H_2O. *Herschel*/HIFI measurements of the line profile of the 1.670-THz transition of H_2O on Jupiter indicated that Comet SL9, rather than IDP, was the principal source of water (Cavalié et al. 2013). The high spectral resolution of *OASIS* will extend this approach to the other Giant Planets. New measurements of Jupiter 35 years after the SL9 impact will enable studies of the meridional transport of H_2O in its stratosphere, thereby constraining dynamical models.

4.3 Inner Solar System

4.3.1 Ceres

The presence and abundance of water in asteroids is relevant to many areas of research, ranging from the origin of water and life on Earth to the large-scale migration of Giant Planets such as Jupiter. HIFI observations of water plumes on Ceres with a production rate of about 6 kg/s pointed to cryo-volcanism (Küppers et al. 2014). Later observations of hazes by the Dawn camera however suggest sublimation of water ice over the Occator crater revealing the presence of material that likely originated from areas beyond the snow line (Nathues et al. 2015). The initial HIFI observations of Ceres provided ambiguous results with 4σ detections in only one polarization and no detection in the other. Repeated observations led to similar results, indicating that the water emission was related to a local source. Finally, 10-hour observations, covering the "light curve"of Ceres led to the crucial detection. The sensitivity of the observation enabled a water production rate of around 1 kg/s to be determined. *OASIS* will increase the sensitivity easily to values below 100 g/s water production rate. This high sensitivity opens a new field of asteroid research. Water emissions may also be found in other asteroids, for instance in carbonaceous chondrites or main belt comets (MBCs). Water sublimation could be one explanation for the observed dust comae in MBCs; however, all attempts to detect water thus far have been unsuccessful (de Val-Borro et al. 2012; O'Rourke et al. 2013) due to the limited sensitivity of existing facilities including *Herschel*/HIFI.

4.3.2 The Moon

The abundance of water on the Moon is of interest both scientifically and for in situ resource utilization (ISRU) as humans return to the Moon for the first time in a half-century. The first evidence for water ice on the Moon came from observations of neutrons from the Lunar Prospector orbiter (Feldman et al. 1998), where neutron flux spectra were interpreted as providing evidence for hydrogen in the form of water ice at the lunar poles. Direct evidence for hydration on the lunar surface was detected by the Moon Mineralogy Mapper on the Chandrayaan-1 orbiter (Pieters et al. 2009), by the EPOXI mission during a lunar flyby (Sunshine et al. 2009), and by *Cassini*/VIMS during its lunar flyby en route to Saturn (Clark 2009). These 3-μm observations showed a mixture of adsorbed water and OH in the lunar regolith. Next, a plume of water and water ice was detected by the LCROSS investigation following the impact of a Centaur rocket near the lunar south pole (Colaprete et al. 2010). Recently, observations conducted from SOFIA detected H_2O in the regolith at 6 μm at high lunar latitudes (Honniball et al. 2021) and the Neutral Mass Spectrometer on the Lunar Atmosphere and Dust Environment Explorer detected exospheric H_2O liberated by meteoroid impacts (Benna et al. 2019). Although water generated from meteoroid impacts is expected to form an H_2O exosphere (Hurley and Benna 2018), the density and spatial variation of the lunar exospheric water remains unknown. The unique vantage point of *OASIS* at the L1 Lagrange point permits high spatial resolution observations of H_2O and OH in the exosphere of the Moon, including the polar regions. *OASIS* will target the 1.670 THz transition of H_2O and the 1.838 THz line of OH. These observations will help determine whether sublimation of water ice contributes to the exosphere or, in contrast, whether the exosphere is present only following meteoroid impacts.

4.3.3 Venus

The upper atmosphere of Venus exhibits large variability in H_2O on time scales of days (Gurwell et al. 2007) to months (Sandor and Clancy 2005). Venus is also highly enriched in HDO, with D/H values ranging from 160 times VSMOW in the lower atmosphere to 240 times VSMOW in the upper atmosphere (Fedorova et al. 2008; Donahue 1999). This has been interpreted as evidence for the loss of a global water ocean due to mass-selective atmospheric escape (Donahue et al. 1997; Donahue 1999), with important implications for past habitability (Way et al. 2016). Recently, Turbet et al. (2021) employed a three-dimensional global climate model that included the effects of atmospheric dynamics and clouds, revealing that oceans may have never existed on Venus' surface. These results suggest that water vapor on Venus never phase changed into liquid water, hindered by strong warming from atmospheric water clouds. OASIS has the ability to map H_2O and HDO as a function of latitude and altitude at a wide range of local times on Venus, which would greatly improve our understanding of the evolution of its atmosphere.

The most detailed study of D/H was performed using the Solar Occultation Infrared spectrometer on the Venus Express mission (Fedorova et al. 2008; Bertaux et al. 2007). H_2O and HDO were measured in absorption against the Sun, at altitudes between 70 and 95 km. The average abundances of H_2O and HDO were 1.2 and 0.09 ppm, respectively, yielding a D/H enrichment of 240 times VSMOW (Fedorova et al. 2008). The solar occultation geometry limited these measurements to the terminator of Venus. In view of the large variability of water, the ability to map H_2O and HDO as a function of latitude and altitude at a wide range of local times would greatly improve our understanding of Venus' atmosphere. Venus' clouds are composed of sulfuric acid; thus, some of the variability in water may be due to

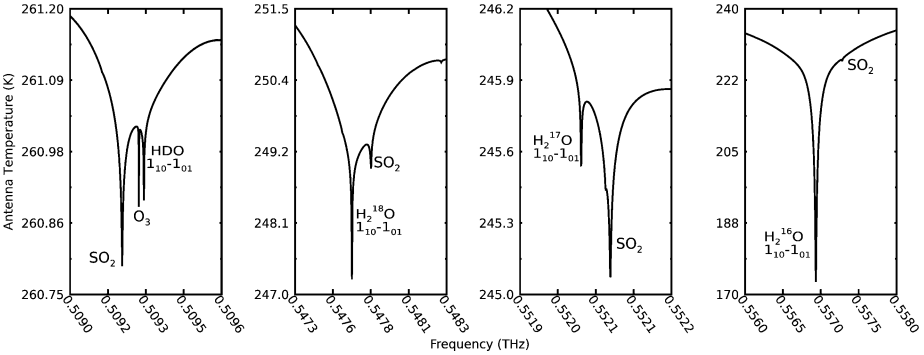

Fig. 13 Venus radiative transfer simulations of its disk-center middle atmospheric absorption of HDO at 0.509 THz (1_{10}-1_{01}), $H_2^{18}O$ at 0.548 THz (1_{10}-1_{01}), $H_2^{17}O$ at 0.552 THz (1_{10}-1_{01}), $H_2^{16}O$ at 0.557 THz (1_{10}-1_{01}), with an O_3 feature and numerous SO_2 features in the spectral vicinities. The *OASIS* beam size spans ∼9-12″ in Band 1. HDO and $H_2^{17}O$ were simulated at a spectral resolution of 100 kHz, while $H_2^{18}O$ and $H_2^{16}O$ were at 3.5 MHz

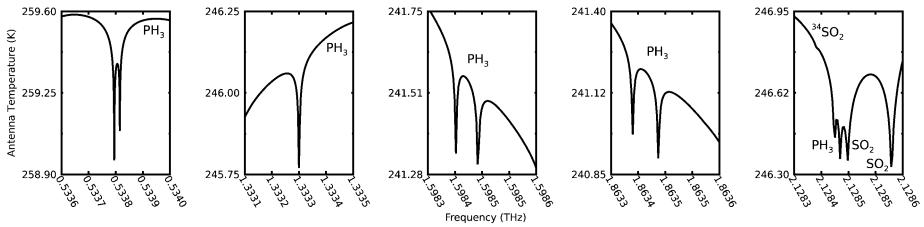

Fig. 14 Venus radiative transfer simulations of its disk-center middle atmospheric absorption of PH_3 at 0.534 THz, 1.333 THz, 1.598 THz, 1.863 THz, and 2.128 THz. The *OASIS* beam size spans ∼9-12″ in Band 1 and ∼2-5″ in Band 2. PH_3 in Band 1 was simulated at a spectral resolution of 100 kHz, while the 4 transitions in Band 2 were at 3.5 MHz

reactions with sulfur compounds (Gurwell et al. 2007). Figure 13 shows a radiative transfer simulation of Venus' middle atmosphere for the 1_{10}-1_{01} transitions of HDO at 0.509 THz, $H_2^{18}O$ at 0.548 THz, $H_2^{17}O$ at 0.552 THz, and $H_2^{16}O$ at 0.557 THz. HDO and $H_2^{17}O$ were simulated at 100 kHz, and their measurement is made possible with the *OASIS* Chirp Transform Spectrometer. While Fig. 13 shows water transitions only in Band 1, numerous transitions exist in Band 2 and Band 4, which also provides higher spatial resolution.

Sulfur compounds are of interest not only for understanding the clouds, but as tracers of either ongoing volcanism (Esposito et al. 1988), or, alternatively, episodic exchanges with the sulfur-rich lower atmosphere (Marcq et al. 2013). Thus, it is important to measure SO_2, SO, OCS, and H_2S to understand these processes (Mills and Allen 2007; Krasnopolsky 2012). A detailed study of Venus Express observations of SO_2 on Venus indicated large variability and an unknown source of sulfur (other than SO_2 and SO) between 70 and 100 km (Vandaele et al. 2017). Recently, ALMA and JCMT observations of Venus led to the unexpected detection of PH_3, which was cited as a potential biosignature (Greaves et al. 2020). Supporting, but not conclusive, evidence for PH_3 was provided by a new study of Pioneer Venus Neutral Mass Spectrometer data (Mogul et al. 2021), although this PH_3 detection has been disputed by several re-analyses of the submillimeter data (Thompson 2021; Villanueva et al. 2021; Akins et al. 2021) and by its absence in infrared spectra (Encrenaz et al. 2020;

Trompet et al. 2021). As indicated in Fig. 14, with the *OASIS* large spectral grasp in Bands 1 and 2, a total of 5 transitions of PH_3 are possible (one in Band 1 and four in Band 2) at 0.534 THz, 1.333 THz, 1.598 THz, 1.863 THz, and 2.128 THz. In view of its significance to both astrobiology and to our understanding of Venus, *OASIS*, with its heterodyne spectral resolution at low frequencies in the submillimeter and far-IR, will be able to confirm (or refute) the controversial detection of PH_3.

Venus is observable from *OASIS* while near its greatest elongation from the Sun (47°), at which time it subtends 25″. The tunability of *OASIS* between 0.465 and 0.557 THz (in Band 1) and between 1.1 and 2.2 THz (in Band 2) will allow us not only to study water and map D/H on Venus, but it will enable the study of PH_3 and numerous sulfur compounds. *OASIS* will be able to measure the latitudinal variation and vertical profile of HDO, H_2O, and sulfur compounds at a wide range of local times on Venus. This will improve our understanding of photochemistry and dynamics in the upper atmosphere. These measurements will build on the successful Venus Express mission, and they will be complementary to in situ measurements from NASA's recently selected DAVINCI Discovery mission to Venus.

OASIS Discovery Science OASIS observations at L1 enable Venus and Earth to be used as ground truth for terrestrial exoplanet analogs. The rich spectrum of the submillimeter and far-IR includes transitions of O_2, O_3, PH_3, CH_4, N_2O, NH_3, OCS, SO, and SO_2, which have been proposed as potential biosignatures despite the fact that abiotic processes on Venus have produced many of these molecules (Krasnopolsky 2012; Meadows et al. 2018; Greaves et al. 2020; Quanz et al. 2019). The abundance of these potential biosignatures on both terrestrial planets will help distinguish an exo-Venus from an exo-Earth when remote sensing spectra of terrestrial exo-planetary atmospheres become available from future space observatories. The submillimeter and far-IR wavelengths covered by OASIS' Bands 1, 2, and 3 provide powerful diagnostics of trace gases that affect the climate systems of terrestrial planets. Numerous exoplanets have been discovered with mass and radii similar to Earth and Venus (Kane et al. 2014, 2019), thus raising hopes for an "Earth-2" in a habitable zone. However, many of these exoplanets may instead more closely resemble the harsh environment of Venus. The unique vantage point at L1 enables OASIS measurements of the abundances of H_2O and CHNOPS-containing molecules contained in the atmospheres of Venus and Earth, paving the way for future remote sensing measurements of terrestrial exoplanets.

5 Baseline and Threshold Observations

In the 1-year Baseline Science Mission, *OASIS* will observe approximately two dozen solar system objects, 6–8 of which are comets. Four JFCs are targeted, and [conservatively] 3–4 OCCs are expected based on consistent discovery rates from ground-based (*e.g.*, PanSTARRS; Morgan et al. 2014) and space-based (*e.g.*, NEOWISE; Mainzer et al. 2014) surveys, the latter demonstrating that ∼7 OCCs 1-km or larger in diameter come within 1.5 AU of the Sun per year (Bauer et al. 2017). For the 6-month Threshold Science Mission, OASIS will observe 8 solar system objects, targeting H_2O and HDO in Europa's atmosphere, in Enceladus' torus, and in two comets (JFCs; 19P and 81P), and HD in the Giant planets, within the first few months of the mission. The observing strategy will employ frequency tuning across OASIS Bands 1-3, necessary to measure at least 5 HDO transitions (*e.g.*, 0.465, 0.490, 0.509, 1.217, 1.625 THz), along with numerous $H_2^{16}O$ (*e.g.*, 0.557, 1.097, 1.670, 2.196 THz), $H_2^{18}O$ (*e.g.*, 0.547, 1.095, 1.656 THz), and $H_2^{17}O$ (*e.g.*, 0.552, 1.662 THz) transitions, plus HD at 2.675 THz. Total observing times will vary depending on the solar system object. For example, comet dwells will take 12 to 24 hrs, the Galilean Moons and Enceladus' torus will require 12-16 hr dwells, and each Giant Planet will take ∼4 hrs.

Acknowledgements T. Cavalié and N. Biver acknowledge support from the CNRS/INSU Programme National de Planétologie (PNP) and CNES.

References

A.B. Akins, A.P. Lincowski, V.S. Meadows et al., Complications in the ALMA detection of phosphine at Venus. Astrophys. J. Lett. **907**(2), L27 (2021). https://doi.org/10.3847/2041-8213/abd56a. arXiv:2101.09831 [astro-ph.EP]

M. Ali-Dib, O. Mousis, J.M. Petit et al., The measured compositions of Uranus and Neptune from their formation on the CO ice line. Astrophys. J. **793**(1), 9 (2014). https://doi.org/10.1088/0004-637X/793/1/9. arXiv:1407.2568 [astro-ph.EP]

K. Altwegg, H. Balsiger, A. Bar-Nun et al., 67P/Churyumov-Gerasimenko, a Jupiter family comet with a high D/H ratio. Science **347**(6220), 1261952 (2015). https://doi.org/10.1126/science.1261952

C.M. Anderson, R.E. Samuelson, R.K. Achterberg et al., Subsidence-induced methane clouds in Titan's winter polar stratosphere and upper troposphere. Icarus **243**, 129–138 (2014). https://doi.org/10.1016/j.icarus.2014.09.007

J.M. Bauer, T. Grav, Y.R. Fernández et al., Debiasing the NEOWISE cryogenic mission comet populations. Astron. J. **154**(2), 53 (2017). https://doi.org/10.3847/1538-3881/aa72df

M. Benna, D.M. Hurley, T.J. Stubbs et al., Lunar soil hydration constrained by exospheric water liberated by meteoroid impacts. Nat. Geosci. **12**(5), 333–338 (2019). https://doi.org/10.1038/s41561-019-0345-3

J.L. Bertaux, D. Nevejans, O. Korablev et al., SPICAV on Venus express: three spectrometers to study the global structure and composition of the Venus atmosphere. Planet. Space Sci. **55**(12), 1673–1700 (2007). https://doi.org/10.1016/j.pss.2007.01.016

N. Biver, D. Bockelée-Morvan, J. Crovisier et al., Radio wavelength molecular observations of comets C/1999 T1 (McNaught-Hartley), C/2001 A2 (LINEAR), C/2000 WM_1 (LINEAR) and 153P/Ikeya-Zhang. Astron. Astrophys. **449**(3), 1255–1270 (2006). https://doi.org/10.1051/0004-6361:20053849

N. Biver, R. Moreno, D. Bockelée-Morvan et al., Isotopic ratios of H, C, N, O, and S in comets C/2012 F6 (Lemmon) and C/2014 Q2 (Lovejoy). Astron. Astrophys. **589**, A78 (2016). https://doi.org/10.1051/0004-6361/201528041. arXiv:1603.05006 [astro-ph.EP]

N. Biver, R. Moreno, D. Bockelée-Morvan, HDO in comet 46P/Wirtanen from ALMA observations (2022, in preparation)

G.L. Bjoraker, Cassini/CIRS observations of water vapor in Saturn's stratosphere (2021, in preparation)

G.L. Bjoraker, S.R. Stolovy, T.L. Herter et al., Detection of water after the collision of fragments G and K of comet Shoemaker-Levy 9 with Jupiter. Icarus **121**(2), 411–421 (1996). https://doi.org/10.1006/icar.1996.0096

D. Bockelée-Morvan, N. Biver, B. Swinyard et al., Herschel measurements of the D/H and $^{16}O/^{18}O$ ratios in water in the Oort-cloud comet C/2009 P1 (Garradd). Astron. Astrophys. **544**, L15 (2012). https://doi.org/10.1051/0004-6361/201219744. arXiv:1207.7180 [astro-ph.EP]

D. Bockelée-Morvan, U. Calmonte, S. Charnley et al., Cometary isotopic measurements. Space Sci. Rev. **197**(1–4), 47–83 (2015). https://doi.org/10.1007/s11214-015-0156-9

L. Bonal, C.M.O.D. Alexander, G.R. Huss et al., Hydrogen isotopic composition of the water in CR chondrites. Geochim. Cosmochim. Acta **106**, 111–133 (2013). https://doi.org/10.1016/j.gca.2012.12.009

P.D. Brown, T.J. Millar, Grain-surface formation of multi-deuterated molecules. Mon. Not. R. Astron. Soc. **240**, 25–29 (1989). https://doi.org/10.1093/mnras/240.1.25P

H.M. Butner, S.B. Charnley, C. Ceccarelli et al., Discovery of interstellar heavy water. Astrophys. J. Lett. **659**(2), L137–L140 (2007). https://doi.org/10.1086/517883

T. Cavalié, H. Feuchtgruber, E. Lellouch et al., Spatial distribution of water in the stratosphere of Jupiter from Herschel HIFI and PACS observations. Astron. Astrophys. **553**, A21 (2013). https://doi.org/10.1051/0004-6361/201220797

T. Cavalié, O. Venot, F. Selsis et al., Thermochemistry and vertical mixing in the tropospheres of Uranus and Neptune: how convection inhibition can affect the derivation of deep oxygen abundances. Icarus **291**, 1–16 (2017). https://doi.org/10.1016/j.icarus.2017.03.015. arXiv:1703.04358 [astro-ph.EP]

T. Cavalié, V. Hue, P. Hartogh et al., Herschel map of Saturn's stratospheric water, delivered by the plumes of Enceladus. Astron. Astrophys. **630**, A87 (2019). https://doi.org/10.1051/0004-6361/201935954. arXiv:1908.07399 [astro-ph.EP]

C. Ceccarelli, C. Dominik, E. Caux et al., Discovery of deuterated water in a young protoplanetary disk. Astrophys. J. Lett. **631**(1), L81–L84 (2005). https://doi.org/10.1086/497028. arXiv:astro-ph/0508256 astro-ph

R.N. Clark, Detection of adsorbed water and hydroxyl on the Moon. Science **326**(5952), 562 (2009). https://doi.org/10.1126/science.1178105

A. Colaprete, P. Schultz, J. Heldmann et al., Detection of water in the LCROSS ejecta plume. Science **330**(6003), 463 (2010). https://doi.org/10.1126/science.1186986

V. Cottini, C.A. Nixon, D.E. Jennings et al., Water vapor in Titan's stratosphere from Cassini CIRS far-infrared spectra. Icarus **220**(2), 855–862 (2012). https://doi.org/10.1016/j.icarus.2012.06.014

A. Coustenis, A. Salama, E. Lellouch et al., Evidence for water vapor in Titan's atmosphere from ISO/SWS data. Astron. Astrophys. **336**, L85–L89 (1998)

A. Coutens, C. Vastel, E. Caux et al., A study of deuterated water in the low-mass protostar IRAS 16293-2422. Astron. Astrophys. **539**, A132 (2012). https://doi.org/10.1051/0004-6361/201117627. arXiv:1201.1785 [astro-ph.GA]

A. Coutens, C. Vastel, S. Cabrit et al., Deuterated water in the solar-type protostars NGC 1333 IRAS 4A and IRAS 4B. Astron. Astrophys. **560**, A39 (2013). https://doi.org/10.1051/0004-6361/201322400. arXiv:1310.7365 [astro-ph.GA]

A. Coutens, C. Vastel, U. Hincelin et al., Water deuterium fractionation in the high-mass star-forming region G34.26+0.15 based on Herschel/HIFI data. Mon. Not. R. Astron. Soc. **445**(2), 1299–1313 (2014). https://doi.org/10.1093/mnras/stu1816. arXiv:1409.1092 [astro-ph.SR]

R.H. Cyburt, B.D. Fields, K.A. Olive et al., Big Bang nucleosynthesis: present status. Rev. Mod. Phys. **88**(1), 015004 (2016). https://doi.org/10.1103/RevModPhys.88.015004. arXiv:1505.01076 [astro-ph.CO]

M. de Val-Borro, L. Rezac, P. Hartogh et al., An upper limit for the water outgassing rate of the main-belt comet 176P/LINEAR observed with Herschel/HIFI. Astron. Astrophys. **546**, L4 (2012). https://doi.org/10.1051/0004-6361/201220169. arXiv:1208.5480 [astro-ph.EP]

N. Dello Russo, H. Kawakita, R.J. Vervack et al., Emerging trends and a comet taxonomy based on the volatile chemistry measured in thirty comets with high-resolution infrared spectroscopy between 1997 and 2013. Icarus **278**, 301–332 (2016). https://doi.org/10.1016/j.icarus.2016.05.039

T.M. Donahue, New analysis of hydrogen and deuterium escape from Venus. Icarus **141**(2), 226–235 (1999). https://doi.org/10.1006/icar.1999.6186

T.M. Donahue, D.H. Grinspoon, R.E. Hartle et al., Ion/neutral escape of hydrogen and deuterium: evolution of water, in *Venus II: Geology, Geophysics, Atmosphere, and Solar Wind Environment*, ed. by S.W. Bougher, D.M. Hunten, R.J. Phillips (1997), p. 385

F. Dulieu, L. Amiaud, E. Congiu et al., Experimental evidence for water formation on interstellar dust grains by hydrogen and oxygen atoms. Astron. Astrophys. **512**, A30 (2010). https://doi.org/10.1051/0004-6361/200912079. arXiv:0903.3120 [astro-ph.IM]

P. Eberhardt, U. Dolder, W. Schulte et al., The D/h ratio in water from comet p/ Halley. Astron. Astrophys. **187**, 435 (1987)

M. Emprechtinger, D.C. Lis, R. Rolffs et al., The abundance, ortho/para ratio, and deuteration of water in the high-mass star-forming region NGC 6334 I. Astrophys. J. **765**(1), 61 (2013). https://doi.org/10.1088/0004-637X/765/1/61. arXiv:1212.5169 [astro-ph.GA]

T. Encrenaz, T.K. Greathouse, E. Marcq et al., A stringent upper limit of the PH_3 abundance at the cloud top of Venus. Astron. Astrophys. **643**, L5 (2020). https://doi.org/10.1051/0004-6361/202039559. arXiv:2010.07817 [astro-ph.EP]

R.I. Epstein, J.M. Lattimer, D.N. Schramm, The origin of deuterium. Nature **263**, 198–202 (1976). https://doi.org/10.1038/263198a0

L.W. Esposito, M. Copley, R. Eckert et al., Sulfur dioxide at the Venus cloud tops, 1978 - 1986. J. Geophys. Res. **93**, 5267–5276 (1988). https://doi.org/10.1029/JD093iD05p05267.

A. Fedorova, O. Korablev, A.C. Vandaele et al., HDO and H_2O vertical distributions and isotopic ratio in the Venus mesosphere by Solar Occultation at Infrared spectrometer on board Venus Express. J. Geophys. Res., Planets **113**(E12), E00B22 (2008). https://doi.org/10.1029/2008JE003146

W.C. Feldman, S. Maurice, A.B. Binder et al., Fluxes of fast and epithermal neutrons from lunar prospector: evidence for water ice at the lunar poles. Science **281**, 1496 (1998). https://doi.org/10.1126/science.281.5382.1496

H. Feuchtgruber, E. Lellouch, T. de Graauw et al., External supply of oxygen to the atmospheres of the giant planets. Nature **389**(6647), 159–162 (1997). https://doi.org/10.1038/38236
H. Feuchtgruber, E. Lellouch, G. Orton et al., The D/H ratio in the atmospheres of Uranus and Neptune from Herschel-PACS observations. Astron. Astrophys. **551**, A126 (2013). https://doi.org/10.1051/0004-6361/201220857. arXiv:1301.5781 [astro-ph.EP]
K. Furuya, Y. Aikawa, H. Nomura et al., Water in protoplanetary disks: deuteration and turbulent mixing. Astrophys. J. **779**(1), 11 (2013). https://doi.org/10.1088/0004-637X/779/1/11. arXiv:1310.3342 [astro-ph.GA]
E.L. Gibb, B.P. Bonev, M.A. DiSanti et al., An infrared search for HDO in comet D/2012 S1 (ISON) and implications for iSHELL. Astrophys. J. **816**(2), 101 (2016). https://doi.org/10.3847/0004-637X/816/2/101
O. Grasset, M.K. Dougherty, A. Coustenis et al., Jupiter ICy moons explorer (JUICE): an ESA mission to orbit Ganymede and to characterise the Jupiter system. Planet. Space Sci. **78**, 1–21 (2013). https://doi.org/10.1016/j.pss.2012.12.002
J.S. Greaves, A.M.S. Richards, W. Bains et al., Phosphine gas in the cloud decks of Venus. Nat. Astron. (2020). https://doi.org/10.1038/s41550-020-1174-4. 2009.06593 [astro-ph.EP]
C.A. Griffith, P. Penteado, K. Baines et al., The evolution of Titan's mid-latitude clouds. Science **310**(5747), 474–477 (2005). https://doi.org/10.1126/science.1117702
M.A. Gurwell, G.J. Melnick, V. Tolls et al., SWAS observations of water vapor in the Venus mesosphere. Icarus **188**(2), 288–304 (2007). https://doi.org/10.1016/j.icarus.2006.12.004
C.J. Hansen, L. Esposito, A.I.F. Stewart et al., Enceladus' water vapor plume. Science **311**(5766), 1422–1425 (2006). https://doi.org/10.1126/science.1121254
P. Hartogh, First direct detection of the water atmospheres of Ganymede and Callisto (2022, in preparation)
P. Hartogh, Y.A. Ilyushin, A passive low frequency instrument for radio wave sounding the subsurface oceans of the Jovian icy moons: an instrument concept. Planet. Space Sci. **130**, 30–39 (2016). https://doi.org/10.1016/j.pss.2016.05.008
P. Hartogh, E. Lellouch, R. Moreno et al., Direct detection of the Enceladus water torus with Herschel. Astron. Astrophys. **532**, L2 (2011a). https://doi.org/10.1051/0004-6361/201117377
P. Hartogh, D.C. Lis, D. Bockelée-Morvan et al., Ocean-like water in the Jupiter-family comet 103P/Hartley 2. Nature **478**(7368), 218–220 (2011b). https://doi.org/10.1038/nature10519
F.P. Helmich, E.F. van Dishoeck, D.J. Jansen, The excitation and abundance of HDO toward W3(OH)/(H_2O). Astron. Astrophys. **313**, 657–663 (1996)
C.I. Honniball, P.G. Lucey, S. Li et al., Molecular water detected on the sunlit Moon by SOFIA. Nat. Astron. **5**, 121–127 (2021). https://doi.org/10.1038/s41550-020-01222-x
S.M. Howell, R.T. Pappalardo, NASA's Europa Clipper—a mission to a potentially habitable ocean world. Nat. Commun. **11**, 1311 (2020). https://doi.org/10.1038/s41467-020-15160-9
D.M. Hurley, M. Benna, Simulations of lunar exospheric water events from meteoroid impacts. Planet. Space Sci. **162**, 148–156 (2018). https://doi.org/10.1016/j.pss.2017.07.008
D. Hutsemékers, J. Manfroid, E. Jehin et al., The ^{16}OH/^{18}OH and OD/OH isotope ratios in comet C/2002 T7 (LINEAR). Astron. Astrophys. **490**(3), L31–L34 (2008). https://doi.org/10.1051/0004-6361:200810833. arXiv:0809.4300 [astro-ph]
Y.A. Ilyushin, P. Hartogh, Submillimeter Wave Instrument radiometry of the Jovian icy moons. Numerical simulation of the microwave thermal radiative transfer and Bayesian retrieval of the physical properties. Astron. Astrophys. **644**, A24 (2020). https://doi.org/10.1051/0004-6361/201937220
E. Jacquet, F. Robert, Water transport in protoplanetary disks and the hydrogen isotopic composition of chondrites. Icarus **223**(2), 722–732 (2013). https://doi.org/10.1016/j.icarus.2013.01.022. arXiv:1301.5665 [astro-ph.EP]
S.S. Jensen, J.K. Jørgensen, L.E. Kristensen et al., ALMA observations of water deuteration: a physical diagnostic of the formation of protostars. Astron. Astrophys. **631**, A25 (2019). https://doi.org/10.1051/0004-6361/201936012. arXiv:1909.10533 [astro-ph.SR]
X. Jia, M.G. Kivelson, K.K. Khurana et al., Evidence of a plume on Europa from Galileo magnetic and plasma wave signatures. Nat. Astron. **2**, 459–464 (2018). https://doi.org/10.1038/s41550-018-0450-z
S.R. Kane, R.K. Kopparapu, S.D. Domagal-Goldman, On the frequency of potential Venus analogs from Kepler data. Astrophys. J. **794**(1), L5 (2014). https://doi.org/10.1088/2041-8205/794/1/l5
S.R. Kane, G. Arney, D. Crisp et al., Venus as a laboratory for exoplanetary science. J. Geophys. Res., Planets **124**(8), 2015–2028 (2019). https://doi.org/10.1029/2019JE005939
C. Kouveliotou, E. Agol, N. Batalha et al., Enduring quests-daring visions (NASA astrophysics in the next three decades) (2014). 1401.3741
V.A. Krasnopolsky, A photochemical model for the Venus atmosphere at 47-112 km. Icarus **218**(1), 230–246 (2012). https://doi.org/10.1016/j.icarus.2011.11.012

M. Küppers, L. O'Rourke, D. Bockelée-Morvan et al., Localized sources of water vapour on the dwarf planet (1)Ceres. Nature **505**(7484), 525–527 (2014). https://doi.org/10.1038/nature12918

E. Lellouch, B. Bézard, T. Fouchet et al., The deuterium abundance in Jupiter and Saturn from ISO-SWS observations. Astron. Astrophys. **370**, 610–622 (2001). https://doi.org/10.1051/0004-6361:20010259

M.C. Liang, B.F. Lane, R.T. Pappalardo et al., Atmosphere of Callisto. J. Geophys. Res., Planets **110**(E2), E02003 (2005). https://doi.org/10.1029/2004JE002322

J.L. Linsky, B.T. Draine, H.W. Moos et al., What is the total deuterium abundance in the local galactic disk? Astrophys. J. **647**(2), 1106–1124 (2006). https://doi.org/10.1086/505556. astro-ph/0608308 [astro-ph]

D.C. Lis, N. Biver, D. Bockelée-Morvan et al., A Herschel study of D/H in water in the Jupiter-family comet 45P/Honda-Mrkos-Pajdušáková and prospects for D/H measurements with CCAT. Astrophys. J. Lett. **774**(1), L3 (2013). https://doi.org/10.1088/2041-8205/774/1/L3. arXiv:1307.6869 [astro-ph.EP]

D.C. Lis, D. Bockelée-Morvan, R. Güsten et al., Terrestrial deuterium-to-hydrogen ratio in water in hyperactive comets. Astron. Astrophys. **625**, L5 (2019). https://doi.org/10.1051/0004-6361/201935554. arXiv:1904.09175 [astro-ph.EP]

S.H. Luszcz-Cook, I. de Pater, Constraining the origins of Neptune's carbon monoxide abundance with CARMA millimeter-wave observations. Icarus **222**(1), 379–400 (2013). https://doi.org/10.1016/j.icarus.2012.11.002. 1301.1990 [astro-ph.EP]

A. Mainzer, J. Bauer, R.M. Cutri et al., Initial performance of the NEOWISE reactivation mission. Astrophys. J. **792**(1), 30 (2014). https://doi.org/10.1088/0004-637X/792/1/30. arXiv:1406.6025 [astro-ph.EP]

M.L. Marconi, A kinetic model of Ganymede's atmosphere. Icarus **190**(1), 155–174 (2007). https://doi.org/10.1016/j.icarus.2007.02.016

E. Marcq, J.L. Bertaux, F. Montmessin et al., Variations of sulphur dioxide at the cloud top of Venus's dynamic atmosphere. Nat. Geosci. **6**(1), 25–28 (2013). https://doi.org/10.1038/ngeo1650

V.S. Meadows, C.T. Reinhard, G.N. Arney et al., Exoplanet biosignatures: understanding oxygen as a biosignature in the context of its environment. Astrobiology **18**(6), 630–662 (2018). https://doi.org/10.1089/ast.2017.1727. 1705.07560 [astro-ph.EP]

R. Meier, T.C. Owen, H.E. Matthews et al., A determination of the HDO/H_2O ratio in comet C/1995 O1 (Hale-Bopp). Science **279**, 842 (1998). https://doi.org/10.1126/science.279.5352.842

F.P. Mills, M. Allen, A review of selected issues concerning the chemistry in Venus' middle atmosphere. Planet. Space Sci. **55**(12), 1729–1740 (2007). https://doi.org/10.1016/j.pss.2007.01.012

R. Mogul, S.S. Limaye, M.J. Way et al., Venus' mass spectra show signs of disequilibria in the middle clouds. Geophys. Res. Lett. **48**(7), e91327 (2021). https://doi.org/10.1029/2020GL091327. 2009.12758 [astro-ph.EP]

R. Moreno, E. Lellouch, L.M. Lara et al., The abundance, vertical distribution and origin of H_2O in Titan's atmosphere: Herschel observations and photochemical modelling. Icarus **221**(2), 753–767 (2012). https://doi.org/10.1016/j.icarus.2012.09.006

J.S. Morgan, W. Burgett, P. Onaka, The Pan-STARRS project in 2014, in *Ground-Based and Airborne Telescopes V*, ed. by L.M. Stepp, R. Gilmozzi, H.J. Hall (2014), p. 91450Y. https://doi.org/10.1117/12.2055680

O. Mousis, A. Aguichine, D.H. Atkinson et al., Key atmospheric signatures for identifying the source reservoirs of volatiles in Uranus and Neptune. Space Sci. Rev. **216**(5), 77 (2020). https://doi.org/10.1007/s11214-020-00681-y. arXiv:2004.11061 [astro-ph.EP]

M.J. Mumma, S.B. Charnley, The chemical composition of comets—emerging taxonomies and natal heritage. Annu. Rev. Astron. Astrophys. **49**(1), 471–524 (2011). https://doi.org/10.1146/annurev-astro-081309-130811

A. Nathues, M. Hoffmann, M. Schaefer et al., Sublimation in bright spots on (1) Ceres. Nature **528**(7581), 237–240 (2015). https://doi.org/10.1038/nature15754

National Academies of Sciences E, Medicine, *Pathways to Discovery in Astronomy and Astrophysics for the 2020s* (Natl. Acad. Press, Washington, 2021). https://doi.org/10.17226/26141. https://www.nap.edu/catalog/26141/pathways-to-discovery-in-astronomy-and-astrophysics-for-the-2020s

National Academies of Sciences E, Medicine, *Origins, Worlds, and Life: A Decadal Strategy for Planetary Science and Astrobiology 2023-2032* (Natl. Acad. Press, Washington, 2022). https://doi.org/10.17226/26522. https://nap.nationalacademies.org/catalog/26522/origins-worlds-and-life-a-decadal-strategy-for-planetary-science

L. O'Rourke, C. Snodgrass, M. de Val-Borro et al., Determination of an upper limit for the water outgassing rate of Main-belt Comet P/2012 T1 (PANSTARRS). Astrophys. J. Lett. **774**(1), L13 (2013). https://doi.org/10.1088/2041-8205/774/1/L13

L. Paganini, M.J. Mumma, E.L. Gibb et al., Ground-based detection of deuterated water in comet C/2014 Q2 (Lovejoy) at IR wavelengths. Astrophys. J. Lett. **836**(2), L25 (2017). https://doi.org/10.3847/2041-8213/aa5cb3

L. Paganini, G.L. Villanueva, L. Roth et al., A measurement of water vapour amid a largely quiescent environment on Europa. Nat. Astron. **4**, 266–272 (2020). https://doi.org/10.1038/s41550-019-0933-6
P.J.E. Peebles, Primordial helium abundance and the primordial fireball. II. Astrophys. J. **146**, 542 (1966). https://doi.org/10.1086/148918
M.V. Persson, J.K. Jørgensen, E.F. van Dishoeck et al., The deuterium fractionation of water on solar-system scales in deeply-embedded low-mass protostars. Astron. Astrophys. **563**, A74 (2014). https://doi.org/10.1051/0004-6361/201322845. arXiv:1402.1398 [astro-ph.SR]
A. Piccialli, R. Moreno, T. Encrenaz et al., Mapping the thermal structure and minor species of Venus mesosphere with ALMA submillimeter observations. Astron. Astrophys. **606**, A53 (2017). https://doi.org/10.1051/0004-6361/201730923
J.D.R. Pierel, C.A. Nixon, E. Lellouch et al., D/H ratios on Saturn and Jupiter from Cassini CIRS. Astron. J. **154**(5), 178 (2017). https://doi.org/10.3847/1538-3881/aa899d
C.M. Pieters, J.N. Goswami, R.N. Clark et al., Character and spatial distribution of OH/H_2o on the surface of the Moon seen by M^3 on Chandrayaan-1. Science **326**(5952), 568 (2009). https://doi.org/10.1126/science.1178658
C. Plainaki, T.A. Cassidy, V.I. Shematovich et al., Towards a global unified model of Europa's tenuous atmosphere. Space Sci. Rev. **214**(1), 40 (2018). https://doi.org/10.1007/s11214-018-0469-6
J.B. Pollack, O. Hubickyj, P. Bodenheimer et al., Formation of the giant planets by concurrent accretion of solids and gas. Icarus **124**(1), 62–85 (1996). https://doi.org/10.1006/icar.1996.0190
C.C. Porco, E. Baker, J. Barbara et al., Imaging of Titan from the Cassini spacecraft. Nature **434**(7030), 159–168 (2005). https://doi.org/10.1038/nature03436
C.C. Porco, P. Helfenstein, P.C. Thomas et al., Cassini observes the active south pole of Enceladus. Science **311**(5766), 1393–1401 (2006). https://doi.org/10.1126/science.1123013
S.P. Quanz, O. Absil, D. Angerhausen et al., Atmospheric characterization of terrestrial exoplanets in the mid-infrared: biosignatures, habitability & diversity (2019). E-prints arXiv:1908.01316 [astro-ph.EP]
L. Roth, J. Saur, K.D. Retherford et al., Transient water vapor at Europa's south pole. Science **343**(6167), 171–174 (2014). https://doi.org/10.1126/science.1247051
B.J. Sandor, R.T. Clancy, Water vapor variations in the Venus mesosphere from microwave spectra. Icarus **177**(1), 129–143 (2005). https://doi.org/10.1016/j.icarus.2005.03.020
V.I. Shematovich, R.E. Johnson, J.F. Cooper et al., Surface-bounded atmosphere of Europa. Icarus **173**(2), 480–498 (2005). https://doi.org/10.1016/j.icarus.2004.08.013
L.A. Soderblom, S.W. Kieffer, T.L. Becker et al., Triton's geyser-like plumes: discovery and basic characterization. Science **250**(4979), 410–415 (1990). https://doi.org/10.1126/science.250.4979.410
J.M. Sunshine, T.L. Farnham, L.M. Feaga et al., Temporal and spatial variability of lunar hydration as observed by the deep impact spacecraft. Science **326**(5952), 565 (2009). https://doi.org/10.1126/science.1179788
M.A. Thompson, The statistical reliability of 267-GHz JCMT observations of Venus: no significant evidence for phosphine absorption. Mon. Not. R. Astron. Soc. **501**(1), L18–L22 (2021). https://doi.org/10.1093/mnrasl/slaa187. arXiv:2010.15188 [astro-ph.EP]
L. Trompet, S. Robert, A. Mahieux et al., Phosphine in Venus' atmosphere: detection attempts and upper limits above the cloud top assessed from the SOIR/VEx spectra. Astron. Astrophys. **645**, L4 (2021). https://doi.org/10.1051/0004-6361/202039932
M. Turbet, E. Bolmont, G. Chaverot et al., Day–night cloud asymmetry prevents early oceans on Venus but not on Earth. Nature **598**(7880), 276–280 (2021). https://doi.org/10.1038/s41586-021-03873-w
E.P. Turtle, J.E. Perry, A.S. McEwen et al., Cassini imaging of Titan's high-latitude lakes, clouds, and south-polar surface changes. Geophys. Res. Lett. **36**(2), L02204 (2009). https://doi.org/10.1029/2008GL036186
E.P. Turtle, A.D. Del Genio, J.M. Barbara et al., Seasonal changes in Titan's meteorology. Geophys. Res. Lett. **38**(3), L03203 (2011). https://doi.org/10.1029/2010GL046266
F.F.S. van der Tak, C.M. Walmsley, F. Herpin et al., Water in the envelopes and disks around young high-mass stars. Astron. Astrophys. **447**(3), 1011–1025 (2006). https://doi.org/10.1051/0004-6361:20053937. arXiv:astro-ph/0510640 [astro-ph]
E.F. van Dishoeck, L.E. Kristensen, J.C. Mottram et al., Water in star-forming regions: physics and chemistry from clouds to disks as probed by Herschel spectroscopy. Astron. Astrophys. **648**, A24 (2021). https://doi.org/10.1051/0004-6361/202039084. arXiv:2102.02225 [astro-ph.GA]
A.C. Vandaele, O. Korablev, D. Belyaev et al., Sulfur dioxide in the Venus atmosphere: I. Vertical distribution and variability. Icarus **295**, 16–33 (2017). https://doi.org/10.1016/j.icarus.2017.05.003
G.L. Villanueva, M.J. Mumma, B.P. Bonev et al., A sensitive search for deuterated water in comet 8p/Tuttle. Astrophys. J. Lett. **690**(1), L5–L9 (2009). https://doi.org/10.1088/0004-637X/690/1/L5
G.L. Villanueva, M. Cordiner, P.G.J. Irwin et al., No evidence of phosphine in the atmosphere of Venus from independent analyses. Nat. Astron. **5**(7), 631–635 (2021). https://doi.org/10.1038/s41550-021-01422-z

J.H. Waite, M.R. Combi, W.H. Ip et al., Cassini ion and neutral mass spectrometer: Enceladus plume composition and structure. Science **311**(5766), 1419–1422 (2006). https://doi.org/10.1126/science.1121290
J.J.H. Waite, W.S. Lewis, B.A. Magee et al., Liquid water on Enceladus from observations of ammonia and ^{40}Ar in the plume. Nature **460**(7254), 487–490 (2009). https://doi.org/10.1038/nature08153
J.H. Waite, R.S. Perryman, M.E. Perry et al., Chemical interactions between Saturn's atmosphere and its rings. Science **362**(6410), aat2382 (2018). https://doi.org/10.1126/science.aat2382
K.S. Wang, F.F.S. van der Tak, M.R. Hogerheijde, Kinematics of the inner thousand AU region around the young massive star <ASTROBJ>AFGL 2591-VLA3</ASTROBJ>: a massive disk candidate? Astron. Astrophys. **543**, A22 (2012). https://doi.org/10.1051/0004-6361/201117044. arXiv:1204.4367 [astro-ph.GA]
W.D. Watson, Ion-molecule reactions, molecule formation, and hydrogen-isotope exchange in dense interstellar clouds. Astrophys. J. **188**, 35–42 (1974). https://doi.org/10.1086/152681
M.J. Way, A.D. Del Genio, N.Y. Kiang et al., Was Venus the first habitable world of our solar system? Geophys. Res. Lett. **43**(16), 8376–8383 (2016). https://doi.org/10.1002/2016GL069790. 1608.00706 [astro-ph.EP]
H.A. Weaver, M.F. A'Hearn, C. Arpigny et al., Atomic deuterium emission and the D/H ratio in comets, in *Asteroids, Comets, Meteors* (2008), p. 8216
L. Yang, F.J. Ciesla, C.M.O.D. Alexander, The D/H ratio of water in the solar nebula during its formation and evolution. Icarus **226**(1), 256–267 (2013). https://doi.org/10.1016/j.icarus.2013.05.027
R.V. Yelle, J.I. Lunine, D.M. Hunten, Energy balance and plume dynamics in Triton's lower atmosphere. Icarus **89**(2), 347–358 (1991). https://doi.org/10.1016/0019-1035(91)90182-S

Authors and Affiliations

Carrie M. Anderson[1] · Nicolas Biver[2] · Gordon L. Bjoraker[1] · Thibault Cavalié[2,3] · Gordon Chin[1] · Michael A. DiSanti[1] · Paul Hartogh[4] · Alexander Tielens[5] · Christopher K. Walker[6]

✉ C.M. Anderson
carrie.m.anderson@nasa.gov

N. Biver
nicolas.biver@obspm.fr

G.L. Bjoraker
gordon.l.bjoraker@nasa.gov

T. Cavalié
thibault.cavalie@u-bordeaux.fr

G. Chin
gordon.chin-1@nasa.gov

M.A. DiSanti
michael.a.disanti@nasa.gov

P. Hartogh
hartogh@mps.mpg.de

A. Tielens
tielens@strw.leidenuniv.nl

C.K. Walker
iras16293@gmail.com

[1] Planetary Systems Laboratory, NASA Goddard Space Flight Center, 8800 Greenbelt Road, Greenbelt, 20771, MD, USA

2 LESIA, Observatoire de Paris, Université PSL, CNRS, Sorbonne Université, Université de Paris, Meudon, France

3 Laboratoire d'Astrophysique de Bordeaux, Univ. Bordeaux, CNRS, B18N, Allée Geoffroy Saint-Hilaire, 33615, Pessac, France

4 Max Planck Institute for Solar System Research, Justus-von-Liebig-Weg 3, Göttingen, Germany

5 Leiden Observatory, P.O. Box 9513, Leiden, The Netherlands

6 Department of Astronomy and Steward Observatory, University of Arizona, 85719, AZ, Tucson, USA